Zwitterionic Surfactant for EOR in Tight Carbonate Reservoir: Physico-Chemical Interaction and Microfluidic Study

by

Zifan Zhang

A thesis submitted in partial fulfillment of the requirements for the degree of

Master of Science

in
Petroleum Engineering

Department of Civil and Environmental Engineering
University of Alberta

Abstract

Recently, during surfactant aided recovery processes for unconventional reservoirs, carboxybetaine based zwitterionic surfactants (C_nDmCB) have attracted attention due to their good tolerance to high saline produced water, remarkable water solubility, and ultra-low interfacial tension (IFT) at extremely low concentrations. The objective of this work is to study the effect of C_nDmCB and C_nDmCB/co-solvents formulations on fluid-fluid and fluid-rock interactions in limestone and tight carbonate reservoirs at varying salinities. More specifically, these interactions correspond to IFT and zeta potential. Additionally, a microfluidic study was conducted to provide insight into the dominating mechanism for tight carbonate reservoirs using different types of surfactants.

The C_nDmCB was prepared using different carbon chain lengths of 12, 14, 16, 18 of tertiary amines and confirmed by ^1H NMR. In turn, the C_nDmCB/co-solvent formulation consists of the previously described formulation plus four small molecular alcohols including 1-butanol, 1-pentanol, isoamyl, 1-octanol with fixed surfactant-to-co-solvent ratio. IFT measurements were initially conducted using the four mentioned surfactants under various concentrations in simulated formation water at varying salinities. Afterwards, the experiment was rerun using surfactant that exhibited the best performance in addition to the co-solvents. Zeta potential test was performed using three surfactants and two surfactants/co-solvents at a wide range of salinities for both the brine/oil and brine/rock systems. These results were compared to the original systems without any additions. Micromodel flood test was conducted in both the water-wet and oil-wet homogeneous porous media as well as the heterogeneous one to visualize the oil displacement pattern of flooding process based on the results of bulk experiments.

Results show that the IFT of C_nDmCB reduces with the increasing carbon chain length except for $C_{18}DmCB$ due to its poor solubilization in the simulated formation water (SFW). The lowest IFT is up to $4.81*10^{-3}$ mN/m magnitude for 0.025 wt% $C_{16}DmCB$ at 100,000 ppm, contributing to the enhanced oil recovery. The additive co-solvents to $C_{16}DmCB$ have adverse effects in terms of IFT, and the magnitude differs from the alkyl chain lengths and structures. The zeta potential of oil droplets remains negative in SFW over the salinity range covered except the salinity of 200,000 ppm. The limestone surface is negatively charged at low salinities after which it becomes positive from 25,000 ppm. However, the surface charge of tight carbonate rock is positive overall due to the extra magnesium ions. Charge conversion from opposite to the same polarity takes place with the presence of all the tested surfactants indicating the potential for altering wettability. C_nDmCB is found not applicable at the low salinity range with the limestone particles. However, the addition of co-solvents to C_nDmCB may improve the magnitude of zeta potential among which $C_{16}DmCB$/1-butanol is suggested. $C_{16}DmCB$ can be used alone considering economic applicability in most other cases with the limestone and tight carbonate samples. In the water-wet homogeneous micromodel, there exists a correlation between ultra-low IFT and higher tertiary oil recovery by the addition of C_nDmCB. However, wettability alteration dominates the early stage while IFT reduction plays an essential role during the late time in the oil-wet porous media.

Preface

This thesis is an original work by Zifan Zhang except the rock analysis presented in Chapter 5, which was done by Dr. Imran Ulhaq. No part of this thesis has been previously published.

My work is dedicated to

My parents

For their endless love, unconditional support and encouragements

Which light my life

Acknowledgements

First and foremost, I would like to show my sincere gratitude to my thesis supervisor, Dr. Japan Trivedi for offering me a great chance to study in his research group which is full of love at the University of Alberta. His ongoing support of academic guidance, encouragement and patient promotes an irreplaceable driving force of my research progress.

Great thanks to Dr. Imran Ulhaq for helping me with the surfactant synthesis. Also thanks to Dr. Madhar Azad for helping me with the thesis writing. The work cannot be completed without their preciseness, kindness and valuable time spent on the instructions.

I would also wish to thank all my friends, colleagues in the research group and my roommate, Ye Liu, who shared their practical suggestions and help throughout the last two years.

Special thanks to my boyfriend, Yice Chen, for his accompany, support and love, which bring sunlight to my life.

Finally, I must express my profound gratitude to my parents, Chunyuan Zhang and Zhengling Zhang, who will always be the person I love the most. This accomplishment would not have been possible without their best love and support.

Table of Contents

List of Tables

List of Figures

Chapter 1: Introduction

1.1 Background

Almost half of the hydrocarbon reserves in the world are carbonate reservoirs, and most of them are fractured, oil-wet or mixed wet (Roehl & Choquette, 2012). The component of crude oil with negative charges absorbs on the positively charged rock surface (Thomas et al., 1993), making the close integration between oil and rock. Only one-third of the original oil can be recovered after waterflooding along with the primary oil recovery due to the special reservoir properties (Siggel et al., 2012; Morvan et al., 2009; Hirasaki et al., 2011; Abramov et al., 2015). Large quantities of oil droplets are still trapped in the pores and struggling to go through the pore throats, which is mainly affected by the capillary force. In oil-wet reservoirs, capillary pressure is not high enough to support spontaneous imbibition. The injected water moves forward to the production well directly with limited imbibition, resulting in even lower oil recovery (Donaldson & Alam, 2013). Thus, wettability alteration from oil-wet to water-wet condition is necessary, which allows the injected solutions to get imbibed into the matrix to displace the trapped oil. Besides, to reduce the residual oil saturation by half, capillary number ought to be increased by 10^3, which can be achieved by reducing interfacial tension (IFT) to ultralow level. Surfactant flooding can either alter the wettability of the rock surface or decrease IFT, hence enhancing the oil recovery.

Many factors have been reported to strongly affect surfactant flooding process, including but not limited to surfactant type, surfactant concentration, reservoir property, additives such as co-solvents or mobility buffer such as polymers (Kamal et al., 2017). Zwitterionic surfactants have attracted attention due to their good tolerance to high saline produced water, remarkable water solubility, ultralow IFT at extremely low concentrations (Zhao et al., 2015; Guo et al., 2015; Kumar & Mandal, 2018). Carboxybetaine based zwitterionic surfactant has better performance according to the literature and will be further studied and analyzed in this work.

1.2 Problem statements and objectives

Previous studies only focused on the influence of surfactants either on the interfacial properties at low salinities or wettability conditions in terms of contact angle on a quartz rock. The objective of this work is to investigate the impacts of carboxybetaine surfactants on both fluid-fluid and fluid-rock interactions at varying salinities on the limestone and tight carbonate rocks, and the effect of co-solvents as additions. Bulk experiments including IFT and zeta potential test were completed with different formulations. Flow experiment in terms of micromodel flood test was conducted based on the best results of previous bulk experiments to determine the dominant mechanism for the enhanced oil recovery in tight carbonate reservoirs. Effect factors including surfactant carbon chain length, surfactant concentration, salinity, carbonate rock type and additive alcohols including 1-butanol, 1-pentanol, isoamyl, 1-octanol as co-solvents were studied. To be more specific, this work aims to answer the following questions:

1. How to synthesize carboxybetaine based zwitterionic surfactants and what's the result of characterization?

2. What's the influence of surfactant alkyl chain length on IFT, and why?

3. What's the effect of surfactant concentration on IFT, and why?

4. What's the implication of salinity on IFT, and which is the recommended salinity in the system?

5. What's the effect of additive co-solvents on IFT, and what's the influence of carbon chain length and structure of the co-solvents?

6. What's the recommended surfactant formulation that gives the lowest IFT under the specific condition?

3

7. What's the original status of brine/oil and brine/rock systems in terms of zeta potential with varying salinities, and how is the wettability condition?

8. What's the influence of additive surfactants to the brine solution on wettability alteration potential with varying salinities?

9. What's the effect of alcohol additions to surfactant solution on wettability alteration potential with varying salinities?

10. What's the influence of different types of carbonate rocks on zeta potential, limestone and tight carbonate in our case, etc.?

11. What's the oil displacement pattern when flooding different formulations, and what's the dominant mechanism that leads to the enhanced oil recovery?

1.3 Thesis outline

Chapter 2 gives a brief introduction of surfactant flooding and emphasizes zwitterionic surfactant flooding through basic conception, action principle and literature review on the experimental methods and results of previous studies.

Chapter 3 shows the synthesis process of the carboxybetaine based zwitterionic surfactants and characterization results obtained from both the actual detection and software prediction.

Chapter 4 demonstrates the methodology and experimental results obtained from interfacial tension measurement. The influence of surfactant alkyl chain length, surfactant concentration, salinity, and additive co-solvents are analyzed, respectively.

Chapter 5 is about the methodology and result analysis of zeta potential test using surfactants with different chain lengths for the brine/oil and brine/rock systems with varying

salinities. Limestone and tight carbonate rocks are studied separately in this section. The effect of additive co-solvents to surfactant solution is also investigated.

Chapter 6 introduces the procedure of the micromodel flood test conducted in both the water-wet and oil-wet porous media. The recorded images of micromodels depict the oil displacement pattern by the injection of different surfactant and surfactant/co-solvent formulations. The dominant mechanism that leads to the higher oil recovery is also analyzed.

Chapter 7 comes to a summary of this work and overall conclusions.

.

Chapter 2:   Literature Review

2.1 Fundamentals of surfactant EOR

2.1.1 Classification of surfactants

In general, a surfactant molecule consists of a polar part which is a hydrophilic head group and a nonpolar part which is a hydrophobic tail making it amphiphilic overall. In surfactant EOR process, the hydrophilic head group interacts with water molecules while the hydrophobic tail penetrates into the oil phase. The amphiphiles absorb on the oil-water interface and typically contribute to the reduction of the interfacial activity. The characteristic of surfactant depends on the hydrocarbon chain length, amount of the branches, functional groups, etc. In terms of the charge of the head group, surfactants are mostly classified into four groups: anionic, cationic, nonionic, zwitterionic.

2.1.1.1 Anionic surfactant

Anionic surfactants are the most generally used surfactants in chemical EOR, which accounts for approximately 50% of surfactants produced. They possess negatively charged head groups and can be mainly classified into three critical types: sulfonates, sulfates, carboxylates (Kamal et al., 2017). Anionic surfactants are potential candidates in sandstone reservoirs but have high adsorption on carbonate rocks due to the ion pair formation between the negative head group and positively charged rock surface. Phase-separate may also happen due to their poor tolerance to high salinity and thermal stability (Zhao et al., 2015; Kamal et al., 2018).

2.1.1.2 Cationic surfactant

Cationic surfactants are well-acknowledged for their available application in carbonate formations because of low adsorption on calcite and other minerals (Ma et al., 2013). Besides, they target more on the mechanism of wettability alteration from oil-wet to water-wet condition due to

the ion-pairs formed by the cationic head groups of surfactant and acidic components of crude oil (Sheng, 2015; Kumar et al., 2016). However, the costs of them are relatively high because they undergo higher pressure hydrogenation reaction during the synthesis process (Sandersen et al., 2012). Standnes and Austad et al. (2000, 2003) demonstrated cationic surfactants were effective in wettability alteration at the concentration above CMC (~1%), but the interfacial tension between oil and water was high. The needed concentration and relatively high IFT necessitate investigating other surfactants (Seethepalli et al., 2004).

2.1.1.3 Nonionic surfactant

Non-ionic surfactants carry no charged group in their heads. They possess good salt tolerance (Abrahamsen, 2012), but the resistant to high temperature is poor. A 'Cloud Point' is found at the temperature where poor dissolution occurs due to the higher thermal energy and weaker hydrogen bonding with the increasing temperature (Zhao et al., 2005). However, this drawback can be improved with the presence of the anionic group, which helps them to resist to high temperature (Ge & Wang, 2015). Furthermore, they have high adsorption in carbonate reservoirs as anionic surfactants, and their IFT reduction capacity is lower than that of ionic surfactants (Kamal et al., 2018; Abrahamsen, 2012).

2.1.1.4 Zwitterionic surfactant

Zwitterionic surfactants, also known as amphoteric surfactants, contain a head with two opposite-charged groups. They have attracted attention due to their good tolerance to high temperature and high salinity, remarkable water solubility, excellent surface properties and thermodynamics at extremely low concentration (Kumar & Mandal, 2018; Lv et al., 2011; Fuseni et al., 2013). Synergistic effect with other ionic surfactants also works well among surfactant mixtures (Zhao et al., 2015). Some of the researchers deal with the zwitterionic surfactants as

nonionic ones because they do not possess net charges (Chevalier et al., 1991; Seredyuk et al., 2001; Blandamer et al., 1995; Matsuno et al., 2010), but others consider them as cationic-like surfactants (Mafi et al., 2016). Table 2.1 shows the name and chemical structural formula of different types of zwitterionic surfactants as well as their synthesis process and experimental results obtained from the corresponding researchers.

Table 2. 1 Different zwitterionic surfactants and corresponding synthesis methodology and properties

Type	Structure	Synthesis Process
Betaine	$\cdot RCHCOO^-$ $^+N(CH_3)_3$	$RCH_2COOH \xrightarrow[ClSO3H]{Cl_2/O_2} RCHCOOH \underset{Cl}{} \xrightarrow{N(CH_3)_3} RCHCOO^- \underset{^+N(CH_3)_3}{}$
Qi et al. (2008) studied the surface activity of alkylbataine zwitterionic surfactants, and they considered them as nonionic ones.		
Carboxybetaine	$H_3C \quad CH_3$ $C_nH_{2n+1} - N - CH_2 - COO^-$	
Kumar and Mandal (2018) investigated carboxybetaine surfactants on quartz rock samples and found them effective in wettability alteration from oil-wet to water-wet. The CMC and IFT decreased with the increasing carbon chain length of the surfactants. Ultra-low IFT around 0.0075 mN/m was observed by the synergistic effect of alkali/C_{16}DmCB at CMC. Results of sand pack flooding showed that the surfactant/polymer/alkali formulation led an additional oil recovery of 30.82% of OOIP.		
Propyl Sulfobetaine	CH_3 $C_nH_{2n+1} - N^+ - CH_2 - CH_2 - CH_2 - SO_3^-$ CH_3	

Zhao et al. (2015) demonstrated that the CMC of propyl sulfobetaine surfactants decreased with the increasing carbon chain lengths and increased with the presence of hydroxyl group. The γ_{CMC} decreased as alkyl chain length increased or by adding hydroxyl group.

Mafi et al. (2016) illustrated the sulfobetaine zwitterionic surfactants were cationic-like because the positively charged group dominated in orienting interfacial water.

Hydroxypropyl Sulfobetaine, Alkyl-hydroxyl-sulfobetaine		
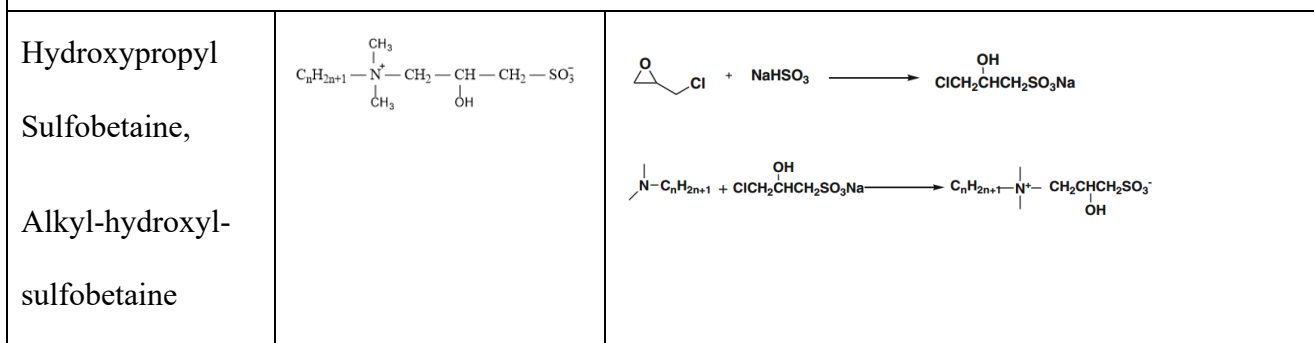
Guo et al. (2015) found the reduction of hydroxyl sulfobetaine surfactant ($C_{18}HSB$) was up to 10^{-3} mN/m using crude oil from different blocks. The formulation of 0.3 wt% $C_{18}HSB$/0.15 wt% HPAM led to 18.6 % improved oil recovery over water flooding.

Zhao et al. (2015) demonstrated that hydroxypropyl sulfobetaine surfactant $C_{14}HSB$ could reach ultralow IFT at the concentration from 0.03 to 0.10wt% under harsh reservoir conditions.

Zwitterionic Gemini Surfactants		
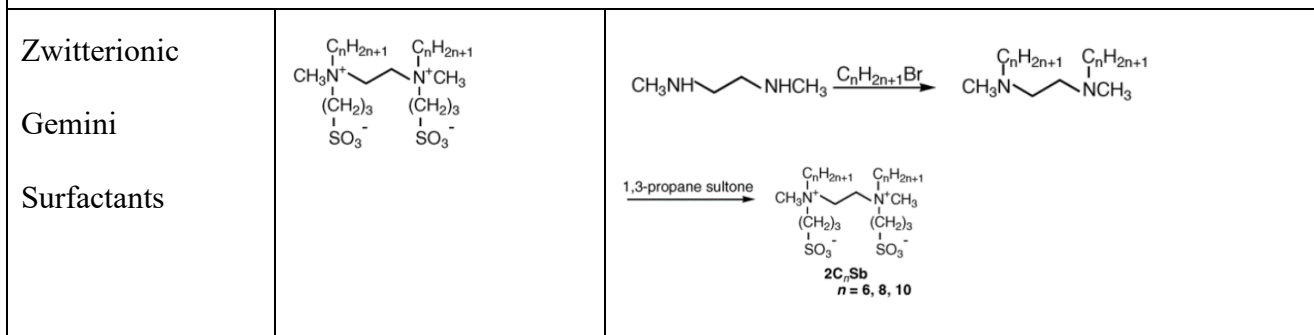
Yoshimura et al. (2006) synthesized sulfobetaine-typed zwitterionic gemini surfactants with the hydrocarbon chain length of 6, 8, 10. Poor water solubilization was found above a certain level of

CMC, but they possessed lower CMC values and surface tension of water. Besides, the surfactant molecules might pack more closely at the air/water interface compared with the monomeric surfactants with the same carbon chain length.

Zwitterionic Gemini Surfactants	
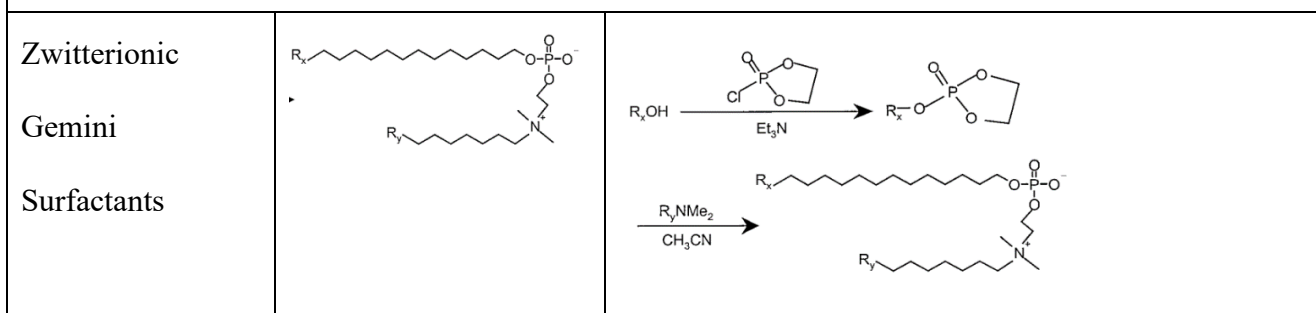
Seredyuk et al. (2001) found that zwitterionic gemini surfactants were able to self-assembled and gave low surface tension at low surfactant concentrations. The molecules might pack efficiently at the interfaces.

Alkanethiol-S-Phosphorylcholine Surfactants	
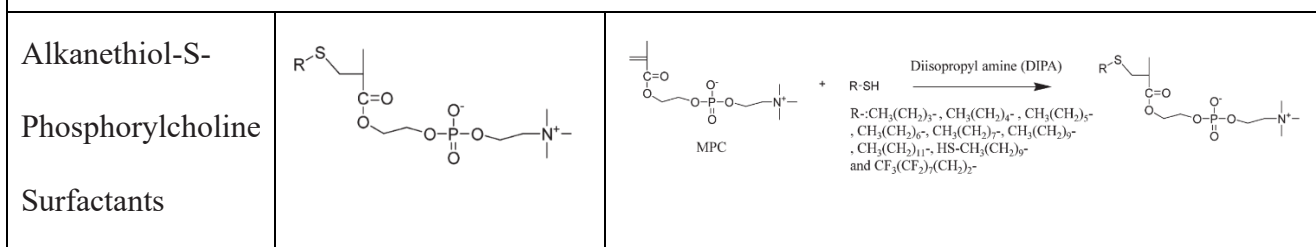
Matsuno et al. (2010) synthesized a library of PC surfactants and investigated the properties of them after which they found these zwitterionic surfactants were similar to nonionic ones in terms of the relation of CMC and carbon number of the surfactants.

2.1.2 Types of reservoir rocks

One petroleum system may consist of one or more reservoir rocks. Types of reservoir rocks depend on the content, composition, sedimentology, etc. The most common sedimentary rocks are made of carbonate or sandstone.

Almost half of the hydrocarbon reserves in the world are carbonate reservoirs, and most of them are fractured, oil-wet or mixed wet (Roehl & Choquette, 2012). This is because the component of crude oil with negative charges absorbs on the positively charged rock surface (Thomas et al., 1993), making the close integration between oil and rock. Carbonate rocks can be further divided into two categories: limestone ($CaCO_3$), which is composed of calcite or aragonite; and dolomites ($CaMg(CO_3)_2$), which is composed of mineral dolomite. In order to avoid high surfactant adsorption on the positively-charged rock surface because of high clay content, cationic or nonionic or mixture surfactants become potential candidates for the solution of precipitation characteristics. But still, inhomogeneity properties of the carbonates lead to lower oil recovery and less effective application (Manrique et al., 2007; Taber et al., 1997). For tight reservoirs, the matrix porosity is less than 10%, and the matrix permeability is usually less than 0.1 millidarcy, which gives rise to more difficulties in the production process.

Sandstones, composed of quartz or feldspar, are initially made of sand with the size between $62\mu m$ to $2mm$. Sandstone reservoirs are homogeneous with relatively high porosity of 10-30% and high permeability, making them good reservoir rocks which are suitable for the application of chemical EOR.

Shale is typically composed of 30% clay minerals and a mass of quartz grains. The size of the grain is smaller than that of sandstone. The permeability of the shale is usually less than 0.1 millidarcy and sometimes 0.001 milliDarcy. The tiny pores within the structure are filled with oil and gas. Thus, the low porosity and ultralow permeability raise problems to recover the oil in the nanopores. Directional drilling and hydraulic fracturing may effectively increase the permeability and produce the oil economically.

2.1.3 Screening criteria

A candidate surfactant should meet several requirements including but not limited to good compatibility and thermal stability under reservoir conditions, the capability of IFT reduction to ultralow level, wettability alteration, low adsorption and retention on the reservoir rocks, compatibility with other chemicals, economic applicability and so on. A large number of surfactants have been investigated through laboratory studies in terms of the characteristics above. Several steps of screening criteria have been used frequently to select the proper surfactant for the specific case. Some of them may be introduced in details in the following sections.

- Compatibility test/Aqueous stability test

- Phase behavior test/Salinity scan test/Puppet test

- Interfacial tension measurement

- Wettability test: contact angle/zeta potential/Amott method/USBM method

- Surfactant adsorption

- Coreflood test/Micromodel flood test

2.2 Mechanism of surfactant flooding

2.2.1 Interfacial tension

After waterflooding, large quantities of oil droplets are still trapped in the pores and struggling to go through the pore throats, which is mainly affected by the capillary force. In order to reduce the resistant to the deformation, interfacial tension should be decreased so that oil droplets can escape more efficiently, resulting in reduced residual oil saturation and enhanced oil recovery. The residual oil saturation is also a function of capillary number indicated by the capillary desaturation curve. Besides, capillary number is a dimensionless parameter defined by

13

the relationship shown in Eq.(1), which is the ratio of viscous force to capillary force. Where, μ is displacing fluid viscosity, u is displacing fluid velocity, σ is interfacial tension between fluids, and θ is contact angle.

$$N_c = \frac{\mu u}{\sigma(\cos \theta)}$$
Eq.(1)

Many studies illuminate the increase in capillary number leads to the reduction of residue oil saturation. For the sake of reducing the residual oil saturation by half, capillary number ought to be increased by 10^3. Since displacing fluid velocity and viscosity cannot be reduced by several magnitudes, IFT is a vital parameter whose reduction can be up to an order of 10^{-3} magnitude which can be achieved by adding surfactants. Surfactant molecules absorb on the oil-water interface and decrease the interfacial tension to an order of 10^{-3} magnitude to overcome the capillary forces. This leads to the mobilization of the trapped residue oil. Hence oil droplets can easily move forward through the pore throats and form oil bank at downstream resulting in higher displacement efficiency (Sheng, 2015). However, it also gives rise to a lower effect on the sweep efficiency because of lower viscosity of the flow fluid. The results of enhanced oil recovery cannot be obtained in terms of the interfacial tension only due to the uncertainty of the multiplication of displacement efficiency and sweep efficiency. An increasing number of studies demonstrate low IFT is not closely related to the highest oil recovery. Ge and Wang (2015) concluded the low IFT was essential but not guaranteed to high oil recovery. Dong et al. (2019) found that the chemical formula selected from emulsification and IFT tests only gave 1.5% improved oil recovery. Thus, it is not enough to study the IFT alone when choosing the optimal surfactant formulations through fluid-fluid interaction. Rock-fluid interaction is also vital, especially in fractured carbonate formations that are mostly oil-wet.

Many factors may influence the value of IFT including but not limited to surfactant characteristics, reservoir properties, additions to the surfactant solutions which will be discussed respectively in this section.

- ■ Surfactant type and structure

The increasing carbon chain length leads to stronger hydrophobic interaction (Guo et al., 2015) or more lipophilic (Gao & Sharma, 2013) in other words, resulting in a preferential movement from the liquid phase to the oil-water interface which makes more surface-active species arrange orderly. Thus, surfactant with larger hydrophobicity is more sufficient in lowering IFT compared to surfactants with a shorter one (Zhao et al., 2008). Since the interfacial energy of -CH_3 group is lower than that of -CH_2 group, the more the -CH_3 group arranged in the outermost layer, the lower the IFT will be obtained (Zhang et al., 2004). Kumar and Mandal (2018) studied the carboxybetaine surfactants with different chain lengths at low salinities and found that the reduction of IFT decreased sharply with increasing carbon chain length from 12 to 16 while the C_{18}DmCB surfactant possessed the largest hydrophobicity and least water solubility. Guo et al. (2015) investigated four alkyl-hydroxyl-sulfobetaine surfactants and found a decrease in IFT as the carbon chain length increased.

- ■ Surfactant concentration

Surfactant concentration is one of the dominant factors that influence IFT results. Surfactant molecules accumulate at the oil-water interface as the concentration increases. There exists a limit where the lowest IFT and corresponding CMC of surfactant are found. Beyond this point, monomers begin to form micelles that decrease the number of monomers from the interface

resulting in higher IFT. Zhao et al. (2015) demonstrated that micelles were produced in both the bulk and oleic phase with the increasing concentration. The solubilization of micelles because of high surfactant concentration led to the consequent decrease in the adsorption capacity of the surface-active species at the interface. Bortolotti et al. (2009) explained the phenomenon by the formation of micelles that led to less effectiveness of IFT reduction. They also found the second low IFT value at higher surfactant concentration attributing to the formation of a stable microemulsion layer. In summary, there should exist an optimal surfactant concentration range for given surfactant, crude oil and reservoir conditions (Zhao et al., 2005).

- Salinity

The concentration of salts also plays an important role in surfactant flooding process. Kumar and Mandal (2018) reported that the value of IFT first decreased and then increased with the increasing salinity based on $C_{16}DmCB$ zwitterionic surfactant solution at CMC. At low salinity range, the solubility of surfactant reduces with the presence of salt, which results in a movement from the bulk phase to the oil-water interface (Bera et al., 2013; James-Smith et al., 2007; Mosayeb & Abedini, 2012; Gao & Sharma, 2013). Higher surfactant adsorption leads to lower IFT. Keeping increasing salinity makes surfactants solubilize more in the oleic phase due to the decreased hydrophilicity and solubility limit. In this case, desorption of surfactant from the interface occurs, resulting in higher IFT (Gupta & Mohanty, 2008). Thus, the optimal salinity is found at which the lowest IFT can be achieved under the specific reservoir condition when surfactant molecules dissolve equally into the bulk and oleic phase (El-Batanoney et al., 1999). Long-chain surfactants may cause phase separation under high salinity while short-chain surfactants have poor oil solubilization at the same condition. Zwitterionic surfactants have been reported to possess the

ability to stand harsh reservoir conditions hence attracting our attention to further study its properties.

- Temperature

Varying results have been reported on the influence of temperature on IFT in surfactant flooding system. Some researchers illustrated that an increase in temperature could enhance the solubility of surfactants (Kamal et al. 2017) and reduce the viscosity of the oil, which supported the movement of surfactant molecules to the oil-water interface (Aoudia et al., 2006). Wu et al. (2010) demonstrated IFT decreased as the temperature increased for 1wt% Alfoterra 35 formulation against n-decane, which was consistent with the above theory. However, Karnanda et al. (2013) found different effects of temperature on the results of IFT. No apparent effects were found when the measurement was conducted with purified water, pure brine and anionic Zonyl FSE. Visible effects were seen with the presence of nonionic surfactants that IFT increased with the increasing temperature for Triton X-100 whereas a decrease was found by the addition of Triton X-405.

- Additive polymer

Polymers are widely used in the oilfield as the addition of surfactant flooding due to surfactant adsorption. Water-soluble polymer molecules uncoil and swell in the brine, resulting in a higher viscosity of the solution. The injection of thickening water reduces the mobility ratio of injected fluid, thus improves sweep efficiency and enhances oil production rates. Among commonly used polymers, polyacrylamides have attracted more attention due to their resistant to temperature and bacteria. Inconsistent results have been reported on the influence of polymers on the IFT. Wu et al. (2015) demonstrated an increase in IFT was found with the presence of polymers

at different concentrations at 30°C, but the magnitude remained at the same level. At a high temperature of 90°C, IFT was reduced at low surfactant concentration while high surfactant concentration made the IFT increase or stay unchanged with the addition of polymer. Some researchers obtained similar results with and without polymers in terms of HPAM and xanthan gum (Hongyan et al., 2009; Nilsson et al., 1997; Pope et al., 1982). Li et al. (2000) illustrated a decrease in IFT due to the decreased dissociation rate of surface-active species, while Taylor & Nasr-El-Din (1996) got similar results above a specific surfactant concentration.

- Additive alkane

The addition of alkali may interact with the acidic component in the crude oil then create in situ surfactant to assist surfactant flooding. Besides, it can also generate foams, improve pH and adjust salinity. The reaction process can be written by Eq.(2). Where HA is component acid, OH^- is alkali component, and A^- is ionized acid. The concentration of ionized acid dominants the alkali effect according to the ratio of ionized to un-ionized species.

$$HA + OH^- \rightleftharpoons A^- + H_2O \hspace{3cm} \text{Eq.(2)}$$

The concentration of ionized species depends on the relative rate of adsorption and desorption. Only if the adsorption rate is higher can the ionized species accumulate at the oil-water interface so that the lowest IFT can be achieved when the ratio is equal to 1 (Kamal et al., 2017). Sheng (2013) demonstrated that adding alkaline into surfactant solutions was equivalently adding salts. Besides, it can change surfactant phase behavior and reduce surfactant adsorption. In Kumar and Mandal's study (2018), the ultralow IFT was found by the synergetic effect of surfactant and alkali. Na_2CO_3 was added to the carboxybetaine surfactant solution at CMC value to investigate the impact of alkali concentration on the IFT of surfactant flooding system. At low alkali

concentrations, in situ surfactants were formed and arranged at the oil-water interface leading to lower IFT. As alkali concentration increased, an increase in ionic strength was found with relatively stable pH value (Xie et al., 2016). This led to a decrease in surfactant formation and an increase in oil solubilization. A movement taken from the oil-water interface to the oleic phase caused a further rise in IFT (Kumar & Mandal, 2018).

However, the deficiencies are also apparent. The presence of alkalis may generate extremely tight emulsions, which are challenging to break, and a costly water softening system is needed for further wastewater treatment. Besides, alkali-assisted surfactant flooding is not suitable for carbonate reservoirs due to precipitation that may damage the reservoir formation.

- ▪ Additive co-solvents or co-surfactants

In surfactant EOR process, surfactant solutions must be single-phase, clear, stable, long-term effective when injecting into the reservoirs, which is necessary to reduce surfactant retention and enhance oil recovery (Dwarakanath et al., 2008; Yang et al. 2010). Co-solvents can be a valid addition assisted in the surfactant flooding process according to the previous studies (Salter, 1977; Salter, 1978; Gogarty & Tosch, 1968). Sahni et al. (2010) illustrated an ASP formulation containing 0.2% Alkyl-aryl sulfonate was cloudy at optimum salinity, but the solution was adequately improved to clear with the presence of hydrophilic co-surfactant and/or co-solvent. Fakhari et al. (2017) found that the gel formation of the poloxamer 407 aqueous solution was disrupted by adding high-concentration ethanol as a co-solvent. Suniga et al. (2016) considered alkoxylated phenols and isobutanol as efficient co-solvents to decrease the viscosity of difficult microemulsions. In summary, the addition of co-solvents aims at minimizing the formation of gels, liquid crystals, viscous phases, reducing the viscosity of microemulsion, and helping achieve aqueous phase stability with lower equilibration time (Sahni et al., 2010; Fakhari et al., 2017;

Suniga et al., 2016). Solubilization problem was observed in zwitterionic surfactant systems reported by other researchers. Guo et al. (2015) studied alkyl hydroxyl sulfobetaine surfactants, whose solubility decreased sharply over the chain length of 18. Kumar and Mandal (2018) found that the IFT reduced with the increasing carbon chain length of carboxybetaine surfactants within a limited level of 16. Therefore, co-solvents may be used as addition along with zwitterionic surfactants for desirable better performance. Among different types of co-solvents, alcohols are considered to be the most commonly used co-solvents in chemical EOR. Small molecular alcohols such as methanol, ethanol, propanol are water-soluble, whose optimal salinity increases with the increasing alcohol concentration. Alcohols of C_6 or larger behaves conversely, and they are assumed to be oil-soluble at all salinities (Salter, 1977). 1-butanol is intermediate-soluble alcohol, which partitions equally into the oil and water phase (Salter, 1977; Shah, 1981). Pei et al. (2014) found isoamyl, 1-pentanol, 1-butanol aided in alkali flooding gave the first three highest improved oil recovery compared with other alcohols. Iglauer et al. (2009) illustrated 1-octanol was the best alcohol generating low interfacial tension in the surfactant system.

Previous studies have put forward different opinions on the influence of alcohols on the value of IFT. Pei et al. (2014) demonstrated an increase in IFT was observed by the addition of small molecular alcohols, notably less water-soluble alcohols such as n-Pentanol and n-Hexanol during alkaline flooding. However, the oil recovery enhanced with the increasing chain length from methanol to n-Pentanol. Sahni et al. (2010) found an increase in hydrophilic co-solvent concentration increased both the optimum salinity and IFT. Inversely, Iglauer et al. (2009) illustrated the IFT reduction by adding n-alcohols with fixed additive concentration (=surfactant+co-solvent) among which 1-Octanol reached the lowest IFT of 0.009 mN/m. It was explained by the synergistic action that the co-solvents packed at the interface decreased the

curvature of the interfacial layer; therefore, reduced the IFT. Pal et al. (2018) concluded that the additive alcohols might increase the mobility of the hydrophobic tail and penetrate deeper into the oil phase. However, oil and water solubilization into the microemulsion phase were decreased. Hence the minimum IFT increased due to the smaller volume of the microemulsion.

2.2.1.2 Measuring techniques

Interfacial tension measurement can be carried out using spinning drop method, pendant drop method and duNouy ring method (Standnes & Austad, 2000).

- ▪ Spinning drop method

Spinning drop method is a commonly used technique carried out by spinning drop tensiometer. The assembly part of the apparatus is a rotational cylinder filled with a dense phase. A droplet of light phase including liquid or gas is injected into the cylinder manually. As the rotation frequency increases, the centrifugal force elongates the droplet until reaching the balance with interfacial tension between two phases. The value of interfacial tension can then be derived from the Eq.(3) with known density contrast and rotation frequency.

$$\gamma = \frac{r^3 \omega^2 (\rho_H - \rho_L)}{4} \qquad \text{Eq.(3)}$$

This is a convenient approach since the curvature at the interface is not necessary to estimate ("Spinning drop method", n.d.), and it is still valid with small quantities of surfactants (Kamal et al., 2017). However, the drawback of this technique is apparent. The results of the test may be highly influenced by the shape of the droplets and the time taken for the stabilization of temperature (Barnes et al., 2008). Furthermore, the results are not accurate for the liquids with high IFT as the centrifugal force is much higher than that of the interfacial tension (Vonnegut, 1942).

- Pendant drop method

Pendant drop method is another approach that can be used for measuring interfacial tension or surface tension. The experimental setup only includes a needle, a camera and a light source (Berry, et al., 2015). The analysis of the drop shape is based on the Young-Laplace equation, Eq.(4), which illustrates the pressure difference between the inside and outside of the curved drop.

$$\Delta P = P_{in} - P_{out} = \sigma \left(\frac{1}{R_1} + \frac{1}{R_2} \right) \qquad \text{Eq.(4)}$$

Two main forces that influence the process is surface tension and gravitation. Surface tension aims to minimize the surface area and seeks to remain the droplet spherical; while gravitation stretches the droplet into pear-like shape ("Pendant drop method", n.d.).

- DuNoüy ring method

DuNoüy ring method is available to measure both the surface tension of the liquid or the interfacial tension between two liquids. The force referred to the wetted length is measured when the ring is lifted slowly from one phase to the other. Then interfacial tension can be obtained from the Eq.(5). Where σ is the surface tension or interfacial tension, F is the maximum force formed when the ring moves through the liquid boundary, L is the wetted length which is the sum of the inner and outer circumference, θ is zero due to the special material of the ring which possesses high surface free energy. It is reported by Krüss company that DuNoüy ring method may not give the surface tension at equilibrium for some samples due to the movement of the ring during the measurement and they suggest wilhelmey plate method as an alternative.

$$\sigma = \frac{F}{L \cos \theta} \qquad \text{Eq.(5)}$$

Another correlation explained by Wikipedia is shown in Eq.(6). Where ω_{ring} is the weight difference of the ring and buoyant force that generated by the portion of the ring below the liquid surface, r_i and r_a are the radius of inner ring and outer ring of the liquid film separately.

$$F = \omega_{ring} + 2\pi(r_i + r_a)\gamma \qquad \text{Eq.(6)}$$

Because the thickness of the ring is much smaller than the diameter, the above equation can be further simplifies into Eq.(7). Where R is the average value of the radius of the inner and outer ring.

$$F = \omega_{ring} + 4\pi R\gamma \qquad \text{Eq.(7)}$$

2.2.2 Wettability alteration

Wettability is defined as 'the tendency of one fluid to spread on or adhere to a solid surface in the presence of other immiscible fluids' (Craig, 1971), which contributes to the distribution and flow of fluids in the reservoir. It describes the preferential tendency of one fluid in contact with a solid rather than another one. The mechanism and application of wettability alteration vary from different types and original conditions of reservoirs. In water-wet reservoirs, water can be imbibed from fractures into the matrix to expel the oil out. In this case, the capillary force is the driving force. The higher the IFT, the greater the driving force, which is beneficial to the oil recovery. However, in oil-wet reservoirs, capillary pressure is not high enough to support spontaneous imbibition. The injected water moves forward to the production well directly with limited imbibition, resulting in even lower oil recovery. Thus, wettability alteration from oil-wet to water-wet condition is also necessary, which allows the injected solutions to get imbibed into the matrix to displace the trapped oil.

2.2.2.1 Mechanisms in different types of reservoirs

- Carbonate reservoirs

Most of the carbonate reservoirs are fractured, oil-wet or mixed wet (Roehl & Choquette, 2012). Wettability alteration in carbonates is a critical process to recover the extra oil in the matrix, which can be accomplished by surfactant flooding.

For cationic surfactants, ion pairs are formed between the cationic head group of the surfactant and ionic component adsorbed on the rock surface. The formation is soluble in the oleic but not aqueous phase. It allows the oil to expel from the matrix by the penetration of the brine. After some of the oil desorbs of the surface, it keeps changing to more water-wet until the limit (Standnes & Austad, 2000).

Anionic surfactants are not able to form ion pairs, but they can generate weak capillary force through hydrophobic interaction. It happens between the lipophilic hydrocarbon tail of surfactant and negatively charged group of crude oil, trying to minimize the contact with the aqueous phase. Thus, the oil may desorb from the carbonates as a consequence of a more water-wet condition.

- Sandstone reservoirs

The circumstance in sandstone reservoirs is more complicated as the rocks varies from strongly water-wet to strongly oil-wet. The wettability mechanism of oil-wet sandstone reservoirs are similar to that of carbonates; however, when the rocks are water-wet, only if the additive surfactants change the wettability to mixed-wet but not oil-wet can surfactant flooding be applicative.

2.2.2.2 Measuring techniques

The process of wettability alteration can be estimated by various approaches including contact angle method, zeta potential method in terms of primary mechanism. Also, Amott method, USBM method, combined Amott-USBM method based on imbibition results will be discussed later.

- Contact angle

In the crude-oil system, wettability can be indicated by the contact angle (θ) between rock surface and an oil droplet placed on it. If $\theta < 90°$, it is more water-wet; if $\theta > 90°$, it is more oil-wet; if $\theta \approx 90°$, it is intermediate-wet or mixed-wet. Imbibition process is driven by capillary pressure defined as Eq.(8). Where σ is IFT between oil and water, θ is contact angle, r is pore radius. If P_c is positive or $\theta < 90°$, spontaneous imbibition takes place to drain the oil out of the core automatically.

$$P_c = \frac{2\sigma \cos \theta}{r} \qquad\qquad \text{Eq.(8)}$$

Contact angle measurement is a relatively cost-friendly technique that usually used in the laboratory work for wettability investigation. It needs a long period to reach equilibrium and wettability may differ from the initial measurement and the equilibrium status after a long time.

- Amott method

Amott method combines spontaneous imbibition and forced displacement measurement together to obtain the wettability preference of the core. It is based on the theory that the wetting phase can imbibe spontaneously into the core that may displace the non-wetting phase. Imbibition increases in the wetting phase, while drainage leads to a reduction in the wetting phase. In the

conventional Amott method, the core saturated with oil is centrifuged under the brine solution until reaching the residual oil saturation. In the modified Amott-Harvey method, the core is centrifuged under brine solution first to reduce the plug to the initial water saturation. Both these two methods include four steps, the order of which depends on the original status of saturation. If the initial sample saturation starts from residual oil saturation, the steps should follow spontaneous oil imbibition, forced oil imbibition, spontaneous water imbibition, forced water imbibition.

The water-wetting index, I_w, or the displacement by brine ratio, δ_w, is calculated by Eq.(9). Where V_{wsi} and V_{wfi} are the the volume of brine imbibed by spontaneous imbibition and forced imbibition respectively. I_w ought to be 1 under completely water-wet condition because spontaneous imbibition almost occupies the the imbibition stage.

$$I_w = \frac{V_{wsi}}{V_{wsi}+V_{wfi}} \qquad \text{Eq.(9)}$$

The oil-wetting index, I_o, or the displacement by brine ratio, δ_o, is calculated by Eq.(10). Where V_{osi} and V_{ofi} are the the volume of oil imbibed by spontaneous imbibition and forced imbibition respectively. I_o ought to be 1 under completely oil-wet condition because spontaneous imbibition almost occupies the the imbibition stage.

$$I_o = \frac{V_{osi}}{V_{osi}+V_{ofi}} \qquad \text{Eq.(10)}$$

The Amott-Harvey wetting index can be referred from Eq.(11). The wettability of the core depends on the value of AHWI that varies from -1 to +1. The result of -0.3 to -1 indicates oil-wet condition; the value of -0.3 to +0.3 represents mixed-wet condition, and +0.3 to +1 means water-wet condition.

$$\text{AHWI} = I_w - I_o \qquad \text{Eq.(11)}$$

Amott method is sensitive at neutral wettability and can be the best method for consolidated cores if forced displacement is performed. Poorly consolidated pores cannot stand the applied force at a high rotational speed. The average wettability of the core can be obtained which is not applicable in the contact angle method.

- USBM method

USBM method consists of primarily forced imbibition and secondary forced drainage process that determines the wettability preference of core plugs. During the primary stage, the plug at the initial water saturation is immersed in the brine and centrifuged at increasing speeds until maximum capillary pressure. Oil production replaced by the brine is recorded and used to calculate the average saturation of the plug. During the secondary stage, the plug at the residual oil saturation is immersed in the oil and centrifuged at increasing speeds until maximum capillary pressure while the volume of the expelled brine is recorded. Capillary pressure is plotted as a function of water saturation for both cases. The ratio of the area under the two capillary curves refers to the wettability index calculated by Eq.(12). Where A_1 and A_2 represents the area under the secondary and primary capillary pressure curves, respectively. A larger A_1 or positive $USBM$ value indicates water-wet condition while a larger A_2 or negative $USBM$ value indicates oil-wet condition. If the two areas are equal to each other, $USBM = 1$ represents mixed-wet status.

$$USBM = log\left(\frac{A_1}{A_2}\right)$$
Eq.(12)

Compared with Amott method, USBM method is more sufficient that can be completed in a few days. It tells the average wettability preference of the plug while the contact angle method can only focus on a localized scale. It is based on industry-standard for comparison of wettability but cannot give accurate results like contact angle method. Similar to Amott method, sample

fracturing may happen due to high rotational speed or a sudden change of the force resulted by stopping or restarting.

- Zeta potential

Rock-fluid interaction can be studied by a variety of methods among which zeta potential test is one of the efficient ways with less limitation. In the dispersed colloidal system, opposite-charged ions around dispersed particles distribute in diffusion state at the interface and form a diffused electric double layer, known as stationary layer. The interface developed by relative movement between the stationary layer and the dispersion medium is termed as slipping plane or shear plane. Zeta potential can be defined as the electric potential at the location of the slipping plane relative to a point in the bulk liquid away from the double layers or potential difference between them (Figure 2.1). Zeta potential is electrokinetic potential, which is a critical indicator of the stability of colloidal dispersion represented by absolute value. The higher the magnitude of the electrostatic repulsion/attraction between suspended particles, the higher the stability of the emulsion. The thickness of water film dominates the stability of it, which depends on the charges of rock surface and brine/oil interface (Hirasaki, 1991).
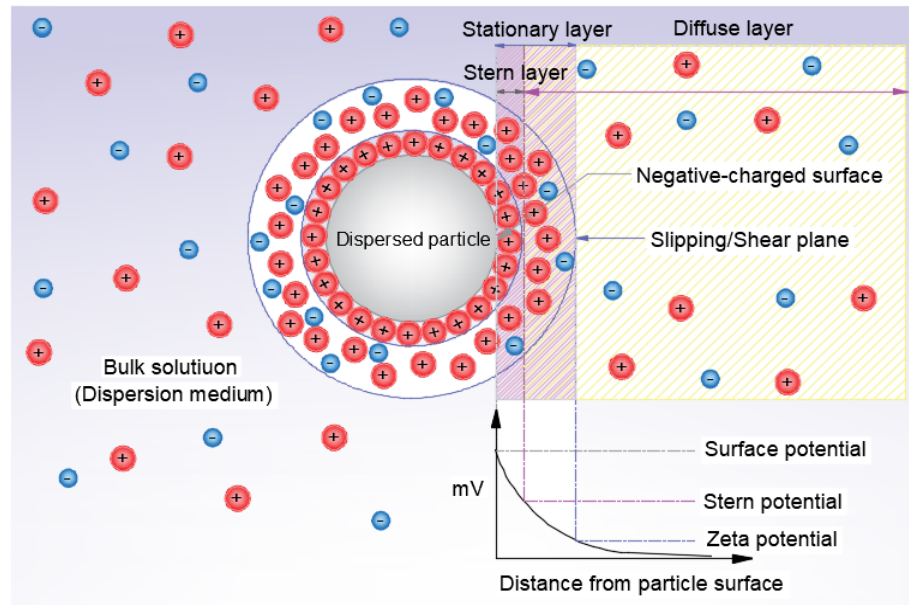
Figure 2. 1 The definition of zeta potential

Rock wettability is a function of both the sign and the magnitude of the electric potentials (Ligthelm et al., 2009; Hirasaki, 1991). Only the same polarity of the brine/rock and brine/oil interface can the repulsive electrostatic force be formed that results in the expansion of the electric double layer and stable/thick water film to generate water-wet rock (Wei et al., 2017; Dubey & Doe, 1993). Zeta potential at the brine/oil interface depends on the salinity, cations and anion types (Quan et al., 2012). It is usually negative under formation conditions (Lager et al., 2008) and tends to be more negative as salinity reduces except for Na_2SO_4 solution (Quan et al., 2012; Alotaibi et al., 2011). If negative charges are observed at the oil-water interface, the injected fluid should also produce negative charges on the rock surfaces and vice versa (Jackson et al., 2016). Alotaibi et al. (2011) demonstrated that changing the surface charges from positive to negative could alter the oil-wet carbonates into water-wet. Mahani et al. (2017) also illustrated the importance of surface-charge alteration and expansion of the electric double layer for higher repulsion force or lower attractive force on the rock surfaces. The changes in the brine/rock system dominated the

mechanism of wettability alteration from oil-wet to water-wet (Mahani et al., 2015; Mahani et al., 2017).

2.3 Surface activities

2.3.1 Surface tension

Surface activities can be indicated by the plot of surface tension as a function of surfactant concentration at a specific temperature. The value of CMC and γ_{CMC} can be estimated from the breakpoints of the curves. The γ_{CMC} indicates the ability of the surfactants to lower surface tensions, and the according CMC illustrates the efficiency. In general, the smaller the CMC value, the superior the surface activity. It can be affected by surfactant types and structures, pressure, temperature, ionic strength, and pH et al (Zhao et al., 2015).

The relationship between the CMC and the alkyl chain length is often described by the empirical equation as Eq.(13) (Zhao et al., 2015). Where A and B are constants and n is the carbon chain length.

$$logCMC = A - Bn \hspace{4cm} \text{Eq.(13)}$$

2.3.2 Surface adsorption

Surfactant adsorption on rock surfaces is a severe problem that cripples the approach for EOR process due to the extra cost generated by additional surfactants. It usually happens between anionic surfactants and carbonate rocks due to ion pair formations.

Surfactant surface adsorption behaviour (Kumar & Mandal, 2018) and the effect of temperature (Zhao et al., 2015) can be compared by parameters such as maximum surface excess concentration(Γ_{max}) and minimum area per surfactant molecule(A_m) at the air-water interface,

which were calculated by Gibbs adsorption isotherm equation (Qi et al., 2008) as shown in Eq.(14) & Eq.(15). Where, n is the solute species, whose concentrations at the interface change with the surfactant concentration C; the value of n is taken as 1 for zwitterionic surfactant in aqueous solution (Zhao et al., 2015; Qi et al., 2008) as most researchers deal with the zwitterionic surfactants as the non-ionic ones for their formally neutral structure (Blandamer et al., 1995; Seredyuk et al., 2001; Chevalier et al., 1991); R is the gas constant equal to $8.314 \, J/(mol \cdot K)$; T is the absolute temperature in Kelvin; N_a is the Avogadro's constant equal to $6.022 \times 10^{23} mol^{-1}$; $d\gamma/dlogC$ is the slope of the plot of surface tension versus log concentration below CMC of surfactant.

$$\Gamma_{max} = -\frac{1}{2.303nRT}\left(\frac{d\gamma}{dlogC}\right)_T \qquad \text{Eq.(14)}$$

$$A_m = \frac{1}{\Gamma_{max}N_a} \qquad \text{Eq.(15)}$$

Thermodynamic is another reason related to the influence of alkyl chain length. The spontaneity of adsorption and micellization behaviour of surfactants can be described using thermodynamic parameters (Zdziennicka & Jańczuk, 2017) as Eq.(16) & Eq.(17) (Kamil & Siddiqui, 2013). Where X_{cmc} is the mole fraction of the surfactant at CMC; π_{cmc} is the surface pressure difference between de-ionized water and surfactant at CMC.

$$\Delta G_{min} = 2.303RTlog(X_{cmc}) \qquad \text{Eq.(16)}$$

$$\Delta G_{ad} = \Delta G_{min} - \frac{\pi_{cmc}}{\Gamma_{max}} \qquad \text{Eq.(17)}$$

2.3.3 Microemulsion and phase behaviour

In the surfactant-brine-oil system, three types of microemulsions would be formed as the salinity increases (Figure 2.2). Surfactants form micelles in either the oleic phase or the aqueous phase depending on the salinity and surfactant hydrophobicity. These micelles solubilize some of the excess oleic or aqueous phases to generate microemulsion, which is a stable dispersion of brine, surfactant, and oil. This multiphase behaviour is called Winsor Types. Winsor type I is termed as oil-in-water microemulsion, in which surfactants form micelles in the brine phase and solubilized a part of excess oil. Winsor type II is known as water-in-oil microemulsion, in which surfactants form micelles in the oil phase and solubilized a portion of excess water. Winsor type III is bi-continuous middle-phase microemulsion, in which equal volume of water and oil solubilize in the microemulsion phase, extending the volume of microemulsion to the maximum. Herein, the value of oil solubilization ratio is the same as the water solubilization ratio, indicating the optimum solubilization ratio and corresponding optimum salinity where the lowest interfacial tension occurs. The salinity of injected water to the system should be close to the optimum salinity (Sheng, 2015). In laboratory study, this evaluation process is salinity scan test, also known as phase behaviour test or puppet test. It helps to understand the interactive behaviours of the components in the system and determine the most substantial volume of microemulsion phase which gives the lowest IFT. An increasing amount of methods can be used to measure phase behaviour, for example, light scattering, turbidity test, visual observation, among which measuring the height of each phase is the most straightforward approach to calculate the amount of each phase. However, it can be substituted by the direct measurement of IFT using equipments.
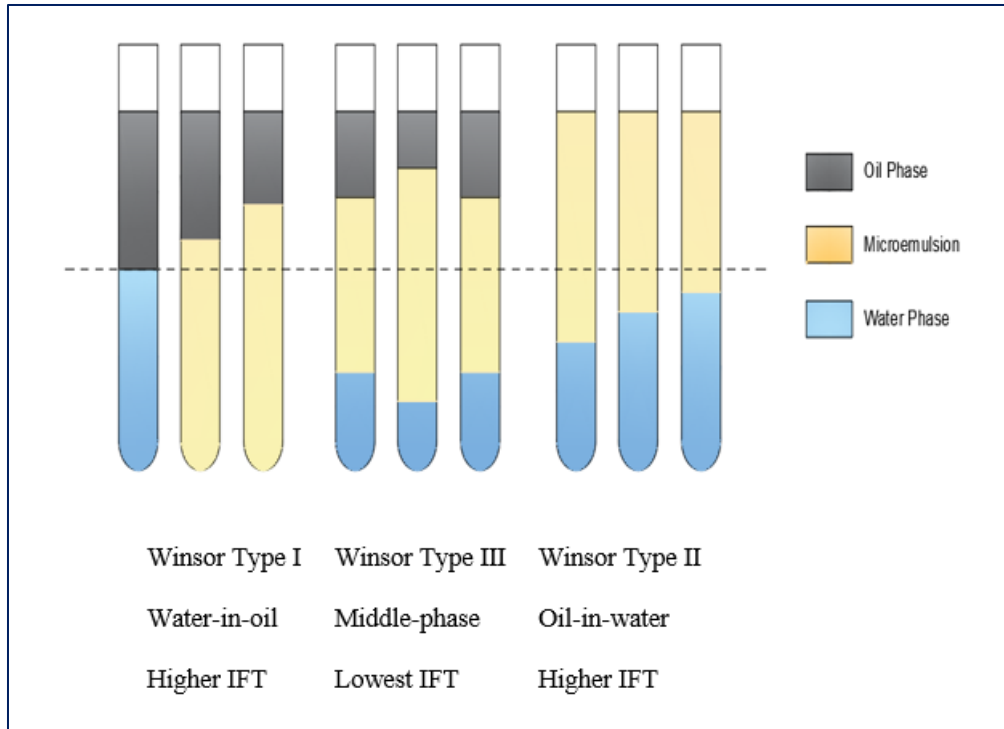
Figure 2. 2 The classification of microemulsion

2.4 Oil recovery

2.4.1 Coreflood test

Coreflood test is a conventional method that determines the efficiency of enhanced oil recovery. The results usually come out with the percentage of original oil in place which represents the total volume of oil reserved in the reservoir before production. The criteria for finding the optimum formulation is not only based on the high ultimate oil recovery but also considering other factors, such as high production rate, early oil breakthrough, high fractional flow of oil, slug size and microemulsion phase behavior (Skauge et al., 1992). Ge and Wang (2015) established the optimized surfactant formulation by mixing a surfactant with the highest ultimate recovery and one with the best recovery rate.

2.4.2 Micromodel flood test

Micromodel flood test is widely used in the evaluation of chemical flooding process to demonstrate the correlation between microscopic displacement mechanism and enhanced oil recovery. The experimental setup for the operation of micromodel flood includes but not limited to an injection pump, a micromodel, a light source and a digital camera.

Pei et al. (2014) used the transparent micromodel made of etched-glass as the porous media to investigate the effect of alcohol on alkaline flooding. The results showed that the additive alcohols enhanced the reaction rate to generate discontinuous W/O droplet flow that improved the sweep efficiency; they also contributed to the viscosity reduction of W/O emulsion which improved the displacement efficiency. Yarveicy & Javaheri (2017) saturated the micromodel with reservoir oil and flooded with brine, solvent, surfactant, microemulsion respectively. The surfactant added to the solution was lauryl betaine, an amphoteric surfactant whose CMC was 320 ppm. Experimental results demonstrated the increasing surfactant concentration led to lower IFT, resulting in higher oil recovery from the micromodel. In Karambeigi's (2015) study, the micromodel was initially saturated with oil followed by water injection as a baseline test after which optimum formulation of emulsion slug was injected continuously. The apparent improvement of sweep efficiency could be observed by the emulsion flooding.

Chapter 3: Surfactant Synthesis

3.1 Materials

For the synthesis of surfactants, N, N-dimethyldodecylamine (>96%), N, N-dimethyltetradecy-lamine (>90%) and N, N-dimethylhexadecylamine (>98%) were purchased from TCI Chemicals (India). N, N-dimethyloctadecylamine (89%), sodium chloroacetate (98%) were procured from Fisher Scientific (Canada). Methanol and de-ionized water were used as solvents during the initial reaction process. Chloroform bought from Sigma-Aldrich (Canada) were used for purification.

3.2 Synthetic methodology

Sodium chloroacetate was mixed with four tertiary amines with different chain lengths in a solvent mixture (Vmethanol:Vwater=1:4) separately. The reactions continued twenty hours under the temperature of 90°C. Figure 3.1 shows the mechanism of the reaction process by corresponding tertiary amines.
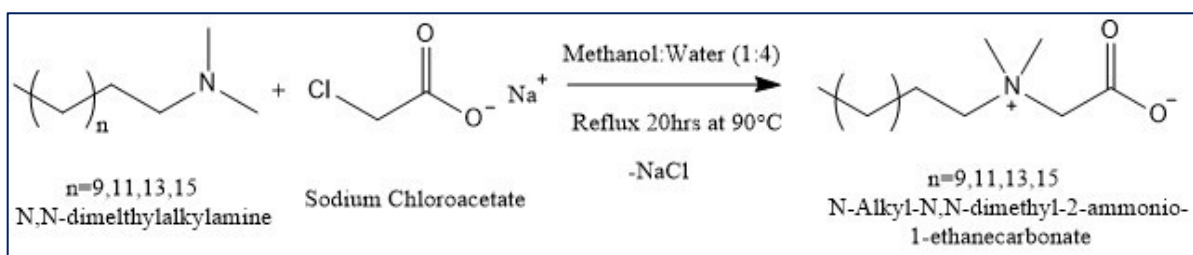
Figure 3. 1 Mechanism of the reaction process for the synthesis of carboxybetaine surfactants

The reactants were added to a round bottom flask with a reflux condenser at the top, which was used to avoid the solvent from boiling away. Attach the tube to the condenser and let the water flow into the tap from the bottom and out of the top. Water droplets could be observed in the condenser and circulated back to the flask (Figure 3.2a).

36
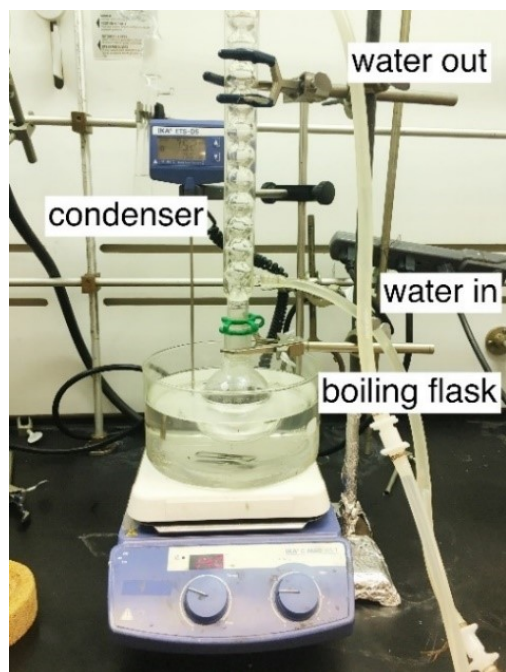
(a)
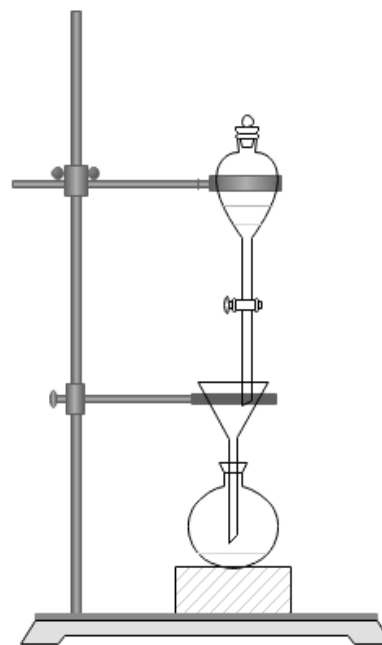
(b)
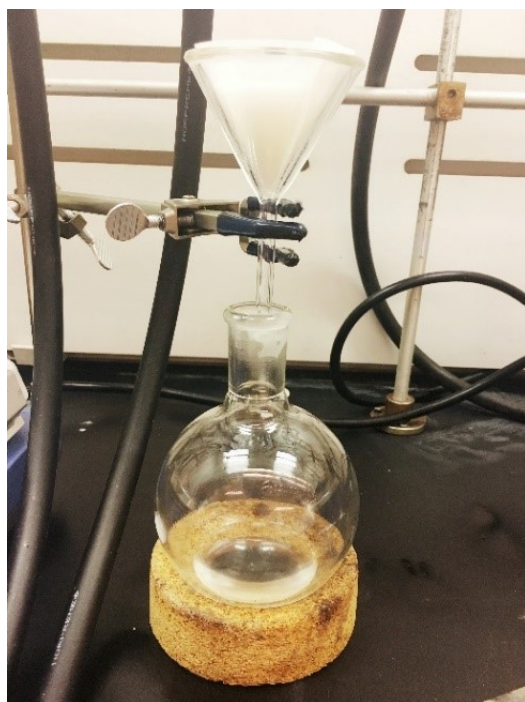
(c)

(d)

Figure 3. 2 (a) Reaction happened in the reflux condenser; (b) Initial filter after dissolving the products by chloroform; (c) Secondary filter to obtain the relatively pure products; (d) Rotavapor R-300

Clear solution or attachment obtained from the reaction was dissolved by the addition of chloroform using magnetic hotplate stirrer. After settling down in a pear-shaped funnel, the solutions showed two layers which the top part was solvents while the bottom portion was used to filter (Figure 3.2b). The filtrate was filtered several times until becoming clear enough (Figure 3.2c). It was then distilled by Rotavapor R-300 whose vacuum was reduced gradually until a mass of bubbles appeared under the temperature of 45°C for about half to one hour (Figure 3.2d). The decreasing pressure aimed at lowering the solvent boiling points, which allowed the solvent to escape more easily. At the same time, the solution was rotated to increase the active area and heated by the water bath to promote the distillation process. The leakage of the products should be avoided by controlling the excessive expansion of the bubbles. The desired products were then obtained by drying under vacuum at 50°C to remove impurities while the reaction time depended on the quantities and chain lengths of the products.

The synthesized surfactants were then characterized by ^{1}H NMR spectroscopy to confirm the proper chemistry structures.

3.3 Characterization

The final products of synthesized surfactants with the increasing carbon chain lengths are all white solid (Figure 3.3). Figure 3.4 And Table 3.1 summarizes the spectral shifts for individual surfactant obtained from Nuclear Magnetic Resonance spectroscopy (^{1}H NMR). The chemical shifts for any type of hydrogen bonds in spectra of samples are almost the same as previous studies (Kumar and Mandal, 2018). The shifts obtained for $COCH_2N+$ demonstrates the reaction happened between reactants. Also, the integration values for $-CCH_2C-$ which increase with the increasing chain lengths roughly verify the successful synthesis. Figure 3.5 depicts the predicted spectral

shifts for both reactant N, N-dimethyldodecylamine (Figure 3.5a) and the reaction product C$_{12}$DmCB (Figure 3.5b) from ChemDraw as one of the examples. Compared with the experiment results, most of the values are similar except a slightly different for that of COCH_2N+. The peaks surrounding 4.396-4.621 occurred during the reaction process. However, the integration kept going down after drying, which indicates the identification of impurities.
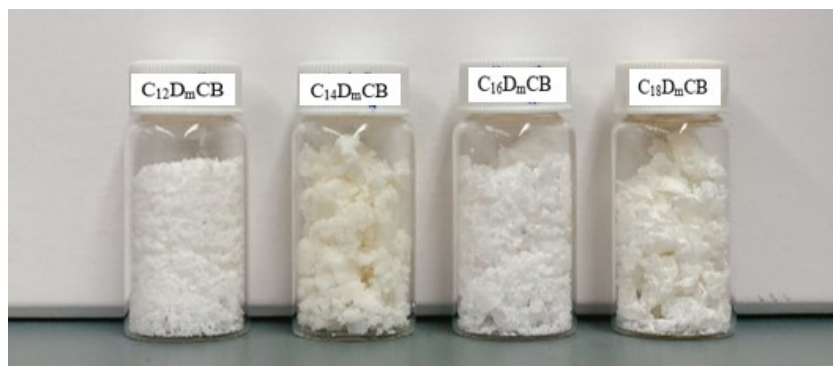
Figure 3. 3 The final state of synthesized surfactants with different alkyl chain lengths
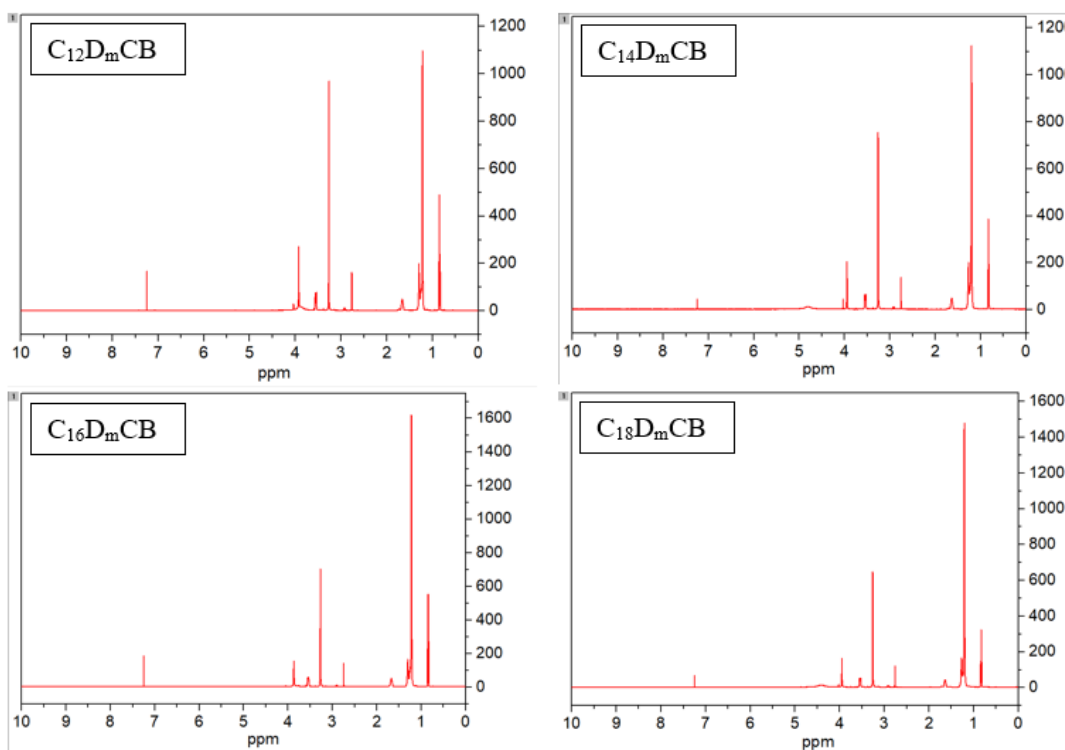
Figure 3. 4 ^{1}H NMR spectra of the synthesized surfactants of different alkyl chain lengths

Table 3. 1 ^{1}H NMR spectra shifts of the synthesized surfactants

Structure	C$_{12}$DmCB	C$_{14}$DmCB	C$_{16}$DmCB	C$_{18}$DmCB
-CH$_2$-CH_3	0.834-0.858	0.813-0.837	0.831-0.855	0.819-0.842
-CCH$_2$C-	1.218-1.291	1.197-1.266	1.219-1.300	1.209-1.270
-CH$_2$CH$_2$N+	1.661	1.636	1.670	1.640
-CH$_2$CH$_2$N+	3.266	3.257	3.268	3.257
CH$_3$N+	3.533-3.562	3.527-3.555	3.531-3.559	3.528-3.556
COCH$_2$N+	3.923	3.947	3.867	3.950
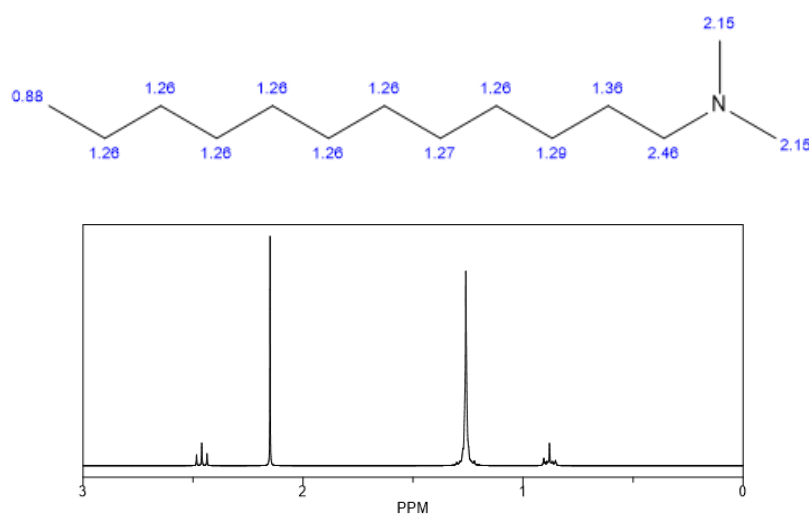
(a)
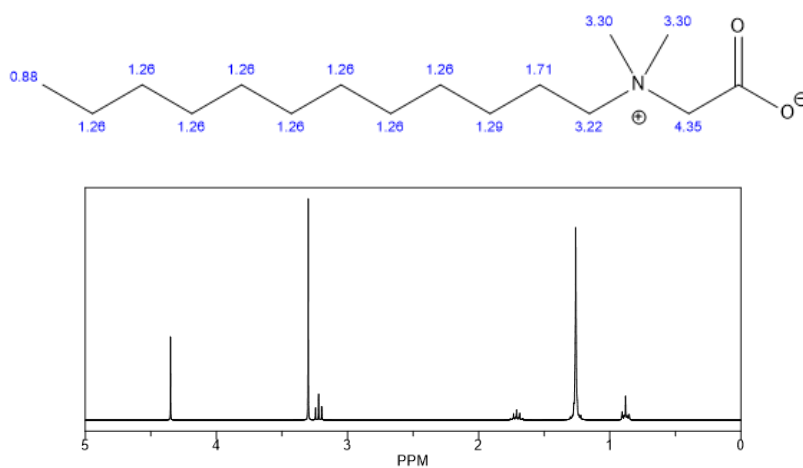
(b)

Figure 3. 5 Predicted spectral shifts for the (a) reactant and (b) reaction product of C$_{12}$DmCB

Chapter 4: Interfacial Tension Measurement

In the case of low permeable reservoirs, higher capillary pressure leads to the poor microscopic displacement efficiency of waterflood. Higher IFT between the injected water and oil is the main reason for the higher capillary pressure. Usually, surfactant solutions are employed to reduce the IFT and increase displacement efficiency. In this chapter, the effect of various zwitterionic surfactants (C_nDmCB) with different alkyl chain lengths on the IFT reduction with the reservoir oil is studied. Further, the effect of the concentration, salinity, co-solvent addition on the interfacial performance of the surfactant is studied.

4.1 Materials

The synthesized surfactants were used after characterization without further treatment. Small molecular alcohols including 1-butanol, 1-pentanol, isoamyl, 1-octanol were procured from Fisher Scientific (Canada). The simulated formation water was prepared in our lab by NaCl, $CaCl_2 \cdot 2H_2O$, $MgCl_2 \cdot 6H_2O$, Na_2SO_4 and $NaHCO_3$, all obtained from Fisher and used without any purification. The composition of the formation water is listed in Table 4.1.

Table 4. 1 The composition of simulated formation water

Components	NaCl	$CaCl_2 \cdot 2H_2O$	$MgCl_2 \cdot 6H_2O$	Na_2SO_4	$NaHCO_3$
Weight Percentage	62%	19.63%	16.3%	1.95%	0.12%

4.2 Methodology

The simulated formation brine was prepared with various salinities of 0, 25,000ppm, 100,000ppm separately. The compounds were mixed and dissolved in the de-ionized water manually and stirred overnight using magnetic stirrer. The referential CMC of $C_{12}DmCB$ obtained from literature was 0.05wt% while the CMC of surfactants with longer chain lengths of 14, 16 and 18 was 0.005wt%. Surfactant concentration started from the referential CMC to twenty times of it

in five times increments were further investigated at varying salinities. Surfactant solutions were stirred using magnetic stirrer until complete dissolution and left overnight to check compatibility. Four small molecular alcohols including 1-butanol, 1-pentanol, isoamyl, 1-octanol were added to the best formulation that generated the lowest IFT as co-solvents with a fixed surfactant-to-alcohol ratio of 1:3.24. IFT measurements were conducted by spinning drop tensiometer SITE100 (Krüss) at ambient temperature. Figure 4.1 depicts the experimental setup of the spinning drop tensiometer and physical structure of the measuring cell, which is an assembly part of the apparatus.

(a)

(b)

(c)
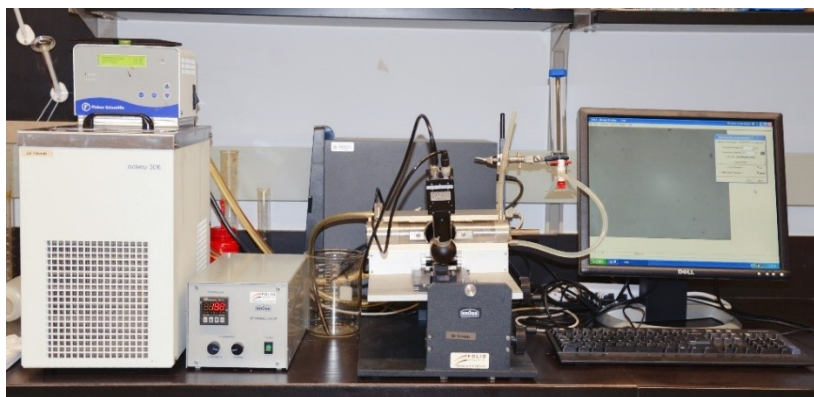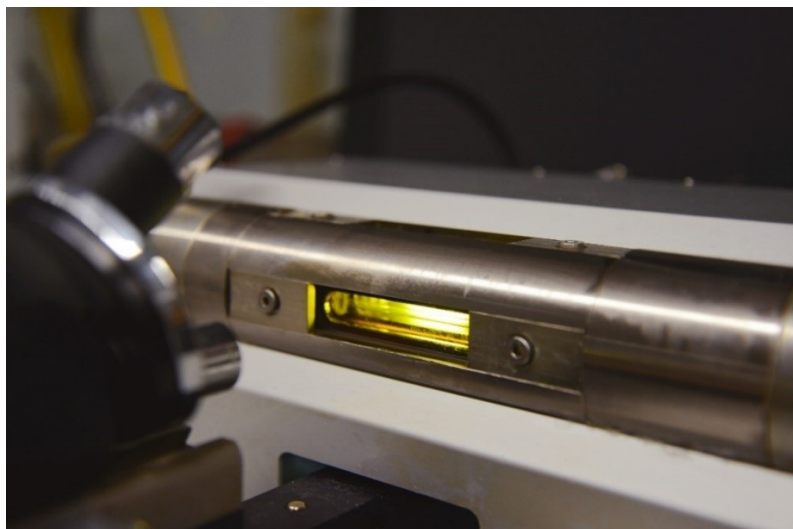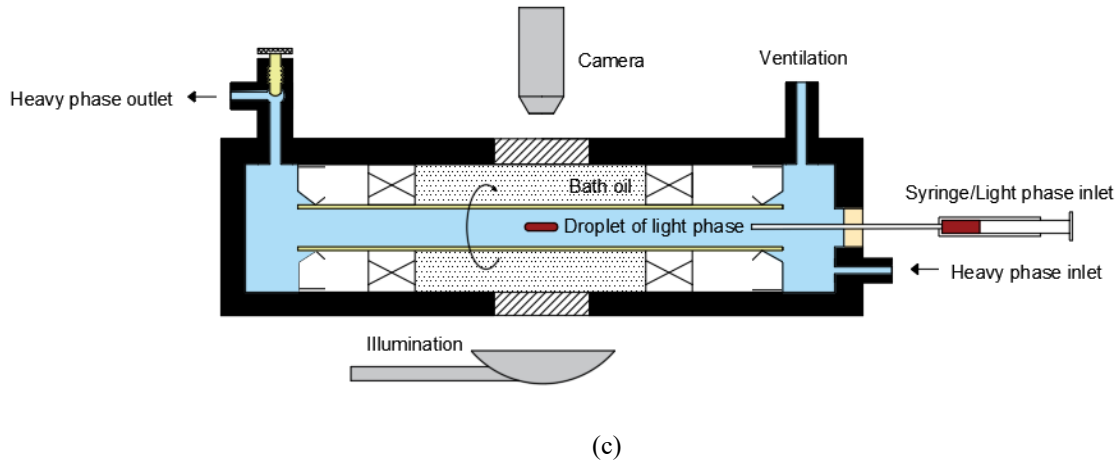
Figure 4. 1 (a) The experimental set up of interfacial tension measurement; (b) The measuring cell as an assembly part of the apparatus; (c) The physical structure of the measuring cell

The rotational cylinder was initially filled with the target solution, and a new calibration of the instrument ought to be created whenever changing the components of the aqueous solution. An oil droplet was then injected into the cylinder manually at the rotation frequency of 1000rpm. As the rotational speed increased to 8000rpm, the centrifugal force elongated the droplet until reaching the balance. Interfacial tension could then be calculated automatically by measuring the drop radius with known densities of oil and brine solutions by Eq. (18).

$$\gamma = \frac{r^3 \omega^2 (\rho_H - \rho_L)}{4} \qquad \text{Eq. (18)}$$

The detailed operation process is listed below:

1. Fill the cylinder with di-water. Open the tap on the cylinder and the outlet valve. Flush the capillary tube with di-water.

2. Close the tap on the cylinder. Close the outlet valve and tilt the platform to the right. Separate the rubber tube which is connected to the measuring cell to remove the water inside the capillary tube.

44

3. Empty and then refill the cylinder with surfactant solution to no more than half way. Connect the rubber tube to the inlet spout, then open the tap on the cylinder. The platform remains slant to fill the tube completely without any residual bubbles.

4. After the same level of liquid is found in the ventilation tube, open the outlet valve until a little liquid flowing out of the tube after which the outlet valve is closed.

5. Move the platform into a horizontal position and open windows-image window in the software.

6. Close the tap on the cylinder. Remove the inlet bushing by unscrewing two outer screws and remove the PTFE sleeve from the capillary.

7. Rinse the needle with di-water. Slowly insert the needle as far as it will go. Adjust the camera to let the needle lies in the middle of the video image. Click 'Calibrate now'.

8. Remove the needle. Reassemble the PTFE bushing and the inlet bushing.

9. Fill in the data with the densities of oil and brine phase, temperature, users, and so on.

10. Open the tap on the cylinder and let the brine solution move forward to fill the capillary tube again. Open the outlet valve and let the liquid flow out a little bit then close the outlet valve.

11. Fill the syringe with the oil. Hold the syringe upright and force residual air out of the syringe and needle.

12. Rotate the capillary at a rotating speed of 1000rpm.

13. Feed the syringe into the syringe guide and pierce the septum with the needle. Dispense a drop into the capillary and move it into the viewing window.

14. Increase the rotating speed step by step from 1000rmp to 8000rmp. Click 'Measure now' to get the results of the measurement.

15. Flush the oil droplet and then change the rotational frequency to 0.

4.3 Results and Analysis

4.3.1 Effect of salinity, alkyl chain length and concentration of C_nDmCB on IFT reduction

The criteria for measuring IFT with spinning drop tensiometer is that lighter phase should be cylindrical. In order to attain the cylindrical shape, the lighter phase elongates with the increasing rotational frequency (Figure 4.2). The lighter phase undergoing elongation at high speed of rotation indicates that surfactant solutions have high IFT. However, the oil phase elongates at relatively very low frequency (1000 rpm) when the surfactant solutions capable of providing ultralow IFT is used.

(a)

(b)

(c)

(d)
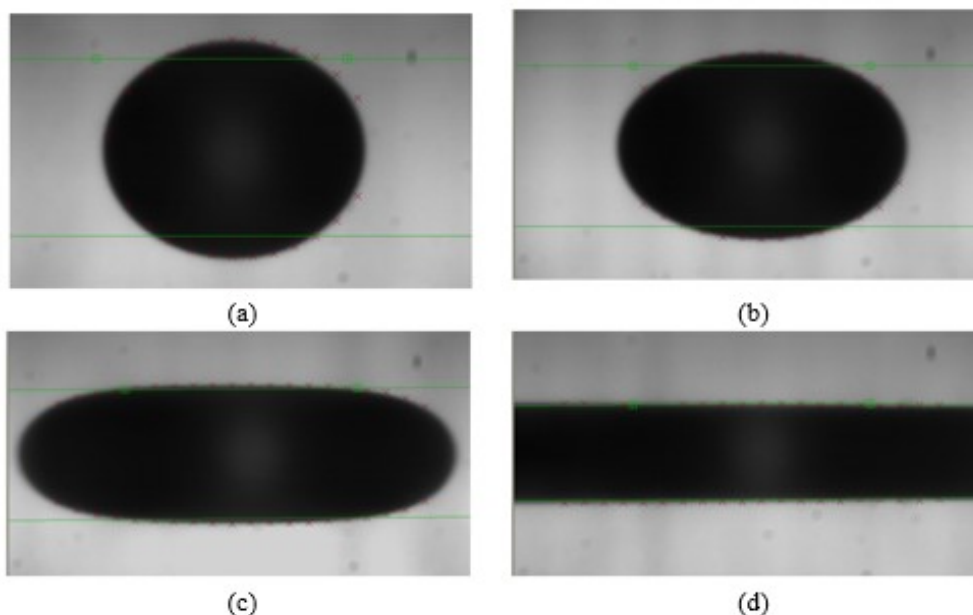
Figure 4. 2 Elongation process of oil droplet at the rotation frequency of (a) 1000rmp; (b) 2000rpm; (c) 4000rpm; (d) 8000rpm separately

With the increase in carbon chain length of C_nDmCB a reduction of solubility is found and the time required for surfactant dissolution increases. However, $C_{18}DmCB$ is insoluble in formation brine. The lowest IFT reduction is up to $4.81*10^{-3}$ mN/m for $C_{16}DmCB$ at the

concentration of 0.025wt% at the salinity of 100,000 ppm (Figure 4.3b). With the increase in time, oil is about to break losing its cylindrical shape (Figure 4.3c) and therefore the IFT value shown in Figure 4.3c is discarded.
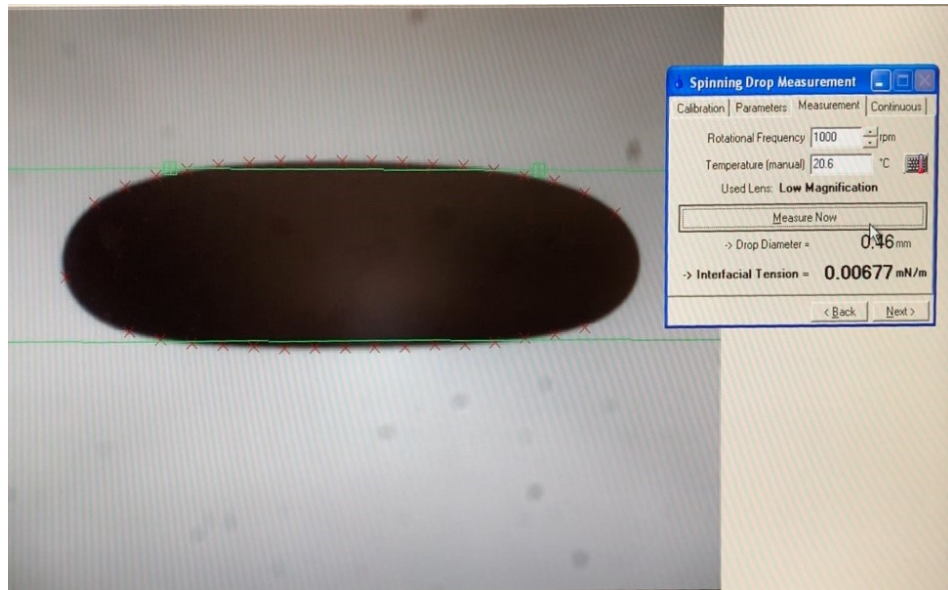
(a)
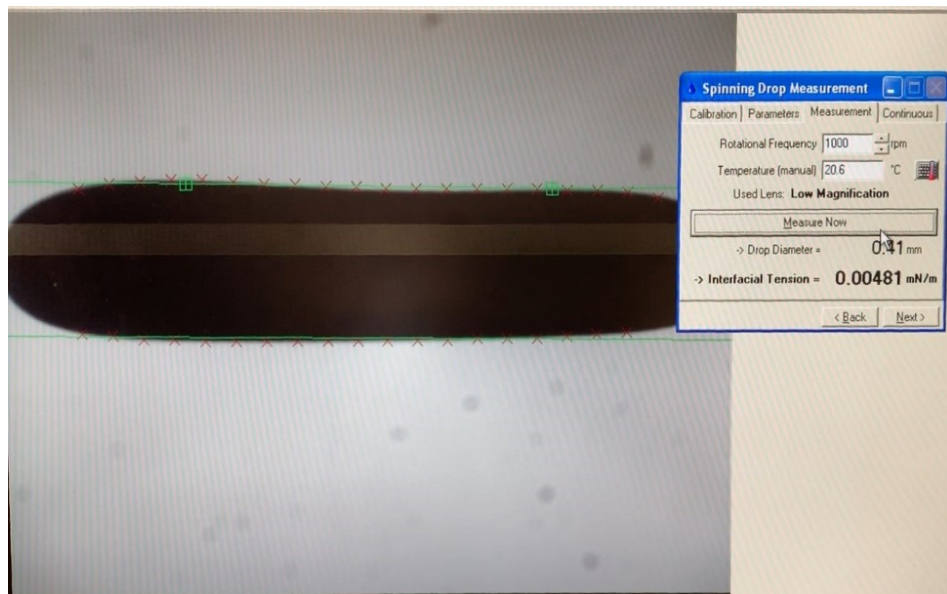
(b)
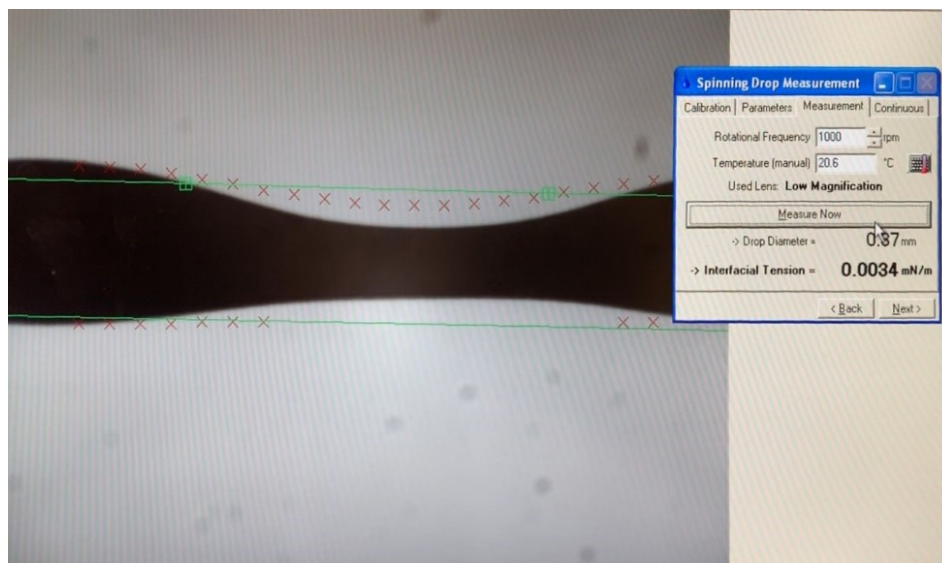
(c)

Figure 4. 3 Deformation process of oil droplet with ultralow IFT for surfactant C_{16}DmCB under the concentration of 0.025wt% at 100,000 ppm (a) Partially elongated oil droplet at 5 seconds; (b) Fully elongated, cylindrical oil droplet at 10 seconds; (c) Oil droplet losing its cylindrical shape after 15 seconds

Figure 4.4 illustrates the equilibrium IFT for different-chain-length surfactants under various surfactant concentrations at varying salinities. While the concentration of C_{14}DmCB and C_{16}DmCB ranged from 0.005 wt% to 0.1 wt%; the concentration of C_{12}DmCB ranged from 0.05 wt% to 1.0 wt%. For all the cases, two salinities of 25,000 ppm and 100,000 ppm were used. Overall, IFT decreases with the increasing carbon chain lengths for most of the tested surfactants except C_{18}DmCB because of its poor solubilization at the studied salinities. The IFT of C_{12}DmCB, C_{14}DmCB and C_{16}DmCB at most of the studied concentrations are around 1 mN/m, 0.1mN/m, 0.01mN/m respectively. IFT of C_{16}DmCB corresponding to a value of 0.01 mN/m implies that increasing the carbon chain length has a beneficial effect on lowering the IFT. Because longer hydrophobic tail penetrates deeper into the oil phase which eventually leads to higher lateral pressure and better interaction with oil (Kumar & Mandal, 2018). Another reason could be an increasing hydrophobic effect that promotes the aggregation and micellization of carboxybetaine

48

molecules (Zhao et al., 2015), making the molecules at the interface more well-organized (Guo et al., 2015). Also, it makes surfactants more lipophilic leading to a movement from bulk aqueous to the oil-water interface (Gao & Sharma, 2013).

For a given salinity, most of the cases show that the IFT decreases first and then goes up or remains unchanged as the surfactant concentration further increases. It should be noted that surfactant behaves differently as free monomers at the oil-water interface and micelles in the brine solution. Only the monomers are the surface-active species which are responsible for the IFT reduction (Singh, 2011). At low concentrations, carboxybetaine molecules remain as monomers. IFT reduces as the number of monomers at the oil-water interface increases. However, monomers begin to aggregate and form micelles after reaching a specific concentration known as CMC. The results show that CMC of the synthesized surfactants are 0.25wt%, 0.025wt%, 0.025wt% respectively.

The effect of salinity is also apparent. Compared with DI water, the presence of salts can reduce the IFT to lower order of magnitude, especially for $C_{16}DmCB$. At low salinity, surfactant molecules partition more into the water phase. As salinity increases, a movement is taken from the water phase to the interface, leading to more surface-active species accumulated (Bera et al., 2013; Gao & Sharma, 2013; El-Batanoney et al., 1999). Another theory can be explained as the synergistic effect of surfactant/salt mixture. The presence of salt thins the layer of the interface and arranges the surfactant molecules at the interface (Zhao et al., 2006; Chu et al., 2004; Zhang et al., 2002; Trabelsi et al., 2012). However, IFT remains at a similar magnitude when the salinity increases to 100,000 ppm. In our case, the brine system with the salinity over 100,000 ppm is unstable due to the diverse types and high concentrations of the composited salts. Hence, 100,000 ppm is considered as the recommended salinity for the injected solution system.

(a)

(b)

50
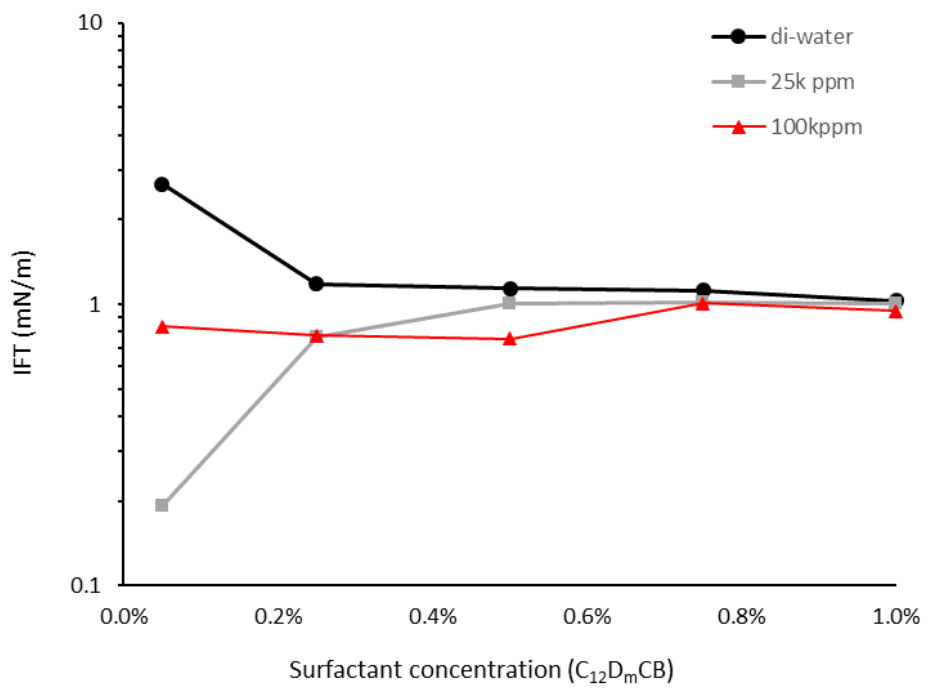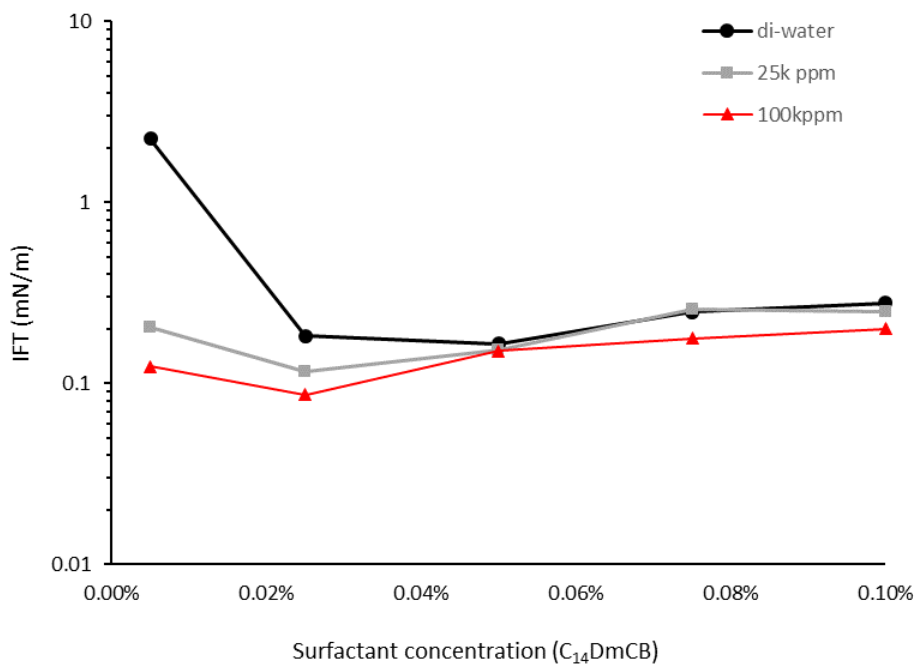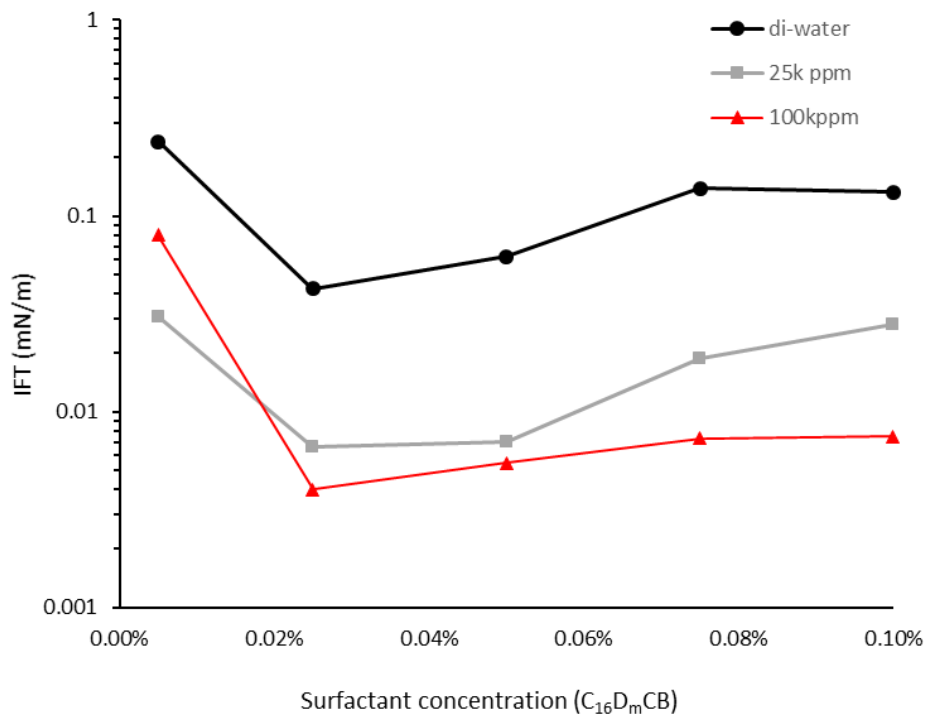
(c)

Figure 4. 4 Equilibrium IFT of different alkyl-chain-length surfactants (a) $C_{12}DmCB$; (b) $C_{14}DmCB$; (c) $C_{16}DmCB$ versus concentration at various salinities

According to the previous studies (Zhao et al.,2015; Kumar & Mandal, 2018) as shown in Table 4.2, three types of zwitterionic surfactants have similar surface tension around 30 mN/m at different CMC. The CMC of hydroxypropyl sulfobetaine is higher than those of others. The hydrogen bond formation between the hydroxyl group and water molecules increases the hydrophilicity (Zhao et al., 2015), leading to higher concentration to form micelles; in other words, higher CMC is observed. Compared our results with the literature, we find that carboxybetaine based zwitterionic surfactants are capable of providing lower IFT at the similar surfactant concentration and salinity. Besides, IFT values of C_nDmCB are more stable over a wide range of surfactant concentration; this is a useful behavior because the formulation may be diluted due to fluid flow in the reservoir (Iglauer et al., 2011). The work of Kumar and Mandal (2018) indicates

that C_nDmCB can perform in the low salinity range of 50 ppm to 500 ppm. In this work, it is shown that C_nDmCB can also perform at the high salinity of 25,000 ppm and 100,000 ppm. Therefore, this surfactant can be used in cEOR process for a wide range of salinities.

Table 4. 2 Comparison among different types of zwitterionic surfactants

Surfactant		CMC (mmol/L)	Salinity (ppm)	IFT (mN/m)	Surfactant concentration at the lowest IFT
propyl sulfobetaine (Zhao et al., 2015)	$C_{12}SB$	1.383	115.2k	0.07-1	0.050%
	$C_{14}SB$	0.233	115.2k	0.06-2	0.050%
	$C_{16}SB$	0.064	115.2k	0.04-2	0.025%
hydroxypropyl sulfobetaine (Zhao et al., 2015)	$C_{12}HSB$	3.389	115.2k	0.04-1	0.050%
	$C_{14}HSB$	0.708	115.2k	0.003-0.4	0.025%
Carboxybetaine (Kumar and Mandal, 2018)	$C_{12}DmCB$	1.84	500	0.1-0.2	0.051%
	$C_{14}DmCB$	0.2	60	0.03-0.04	0.006%
	$C_{16}DmCB$	0.15	50	0.009-0.04	0.005%
Carboxybetaine	$C_{12}DmCB$	-	100k	0.7-1.0	0.250%
	$C_{14}DmCB$	-	100k	0.08-0.18	0.025%
	$C_{16}DmCB$	-	100k	0.004-0.08	0.025%

4.3.2 Effect of co-solvent additions to $C_{16}DmCB$

Based on the IFT results (Figure 4.4), $C_{16}DmCB$ is found to be the optimal one for lowering the IFT. Thus, $C_{16}DmCB$ is chosen for further study in the presence of alcohol. Alcohols of different chain lengths and structures including 1-butanol, 1-pentanol, isoamyl, and 1-octanol are considered in this study. After stirring for 12 hours, most surfactant/alcohol formulations resulted

in clear solutions. However, it took 72 hours to get a clear solution with 1-octanol. Figure.4.5 shows the impact of additive alcohols on the IFT of the chosen surfactant. Overall, the equilibrium IFT increases by the addition of n-alcohols. These intermediate or oil-soluble alcohols partition equally or more into the oil phase. A preferential movement of the alcohol molecules taken from the bulk phase to the oleic phase occupies the spaces at the oil-water interface. Thus, IFT increases as the number of surface-active species reduce.

Addition of various types of alcohol to surfactant results in different interfacial behaviors. From Figure 4.5, it is clear that 1-butanol, an intermediate-soluble alcohol doesn't change the IFT of $C_{16}DmCB$ much. Whereas, the addition of 1-pentanol to the surfactant drastically increases the IFT of the $C_{16}DmCB$ from $4.81*10^{-3}$ mN/m to 0.0228 mN/m (Figure 4.5). This is attributed to the higher oil-soluble property of 1-pentanol, resulting in the occupation of more alcohol molecules at the oil-water interface during the movement from the water phase to the oleic phase. The result is consistent with the previous studies conducted by Pei et al. (2014) by adding different types of 0.5wt% low molecular alcohols to 0.5wt% NaOH solution. The work illustrated less water-soluble alcohol provided higher alcohol concentration at the interface, thus reduced the number of surfactant species. A few differences are found between 1-pentanol and isoamyl, which has the same carbon chain length but different structures. The IFT of the surfactant solution with the presence of isoamyl is lower than that of 1-pentanol because it has one more $-CH_3$ group and less $-CH_2$ group. The interfacial energy of $-CH_3$ group is smaller so that the more the $-CH_3$ group, the lower the IFT (Zhang et al., 2004). A sharp rise in IFT is found by the presence of 1-octanol. 1-octanol is insoluble in the water phase but can be miscible in the oil phase so that most of the alcohol molecules move to the oleic phase and occupy the oil-water interface during the movement. However, in Iglauer's (2009) work, 1-octanol had the maximum capacity for generating low IFT

among tested alcohols (1-propanol, 1-butanol, and 1-Hexanol) when combined with alkyl polyglycosides (APG), a nonionic carbohydrate-based surfactant. In our study, due to the poor solubilization and relatively high IFT generated, 1-octanol is not a potential candidate.

It is reported by several researchers that the function of alcohols can also be influenced by the relative chain length of the surfactants and alcohols (Pei et al., 2014; Zhang et al., 2004). If the alkyl chain lengths of alcohols are much shorter than that of surfactants, the functions of $-CH_3$ group may be reduced since the alcohol is hidden by the long-chain surfactant (Zhang et al., 2004). Thus, the difference of IFT between 1-pentanol and the isoamyl-assisted system is not significant. In our case, the carbon chain length of surfactant is four times of the alcohols'. Alcohols with shorter chain lengths possess a higher chance to be covered by the chains of surfactants; thus lower molecular alcohols do not change the value of IFT a lot while 1-octanol leads to a sharp increase in IFT.
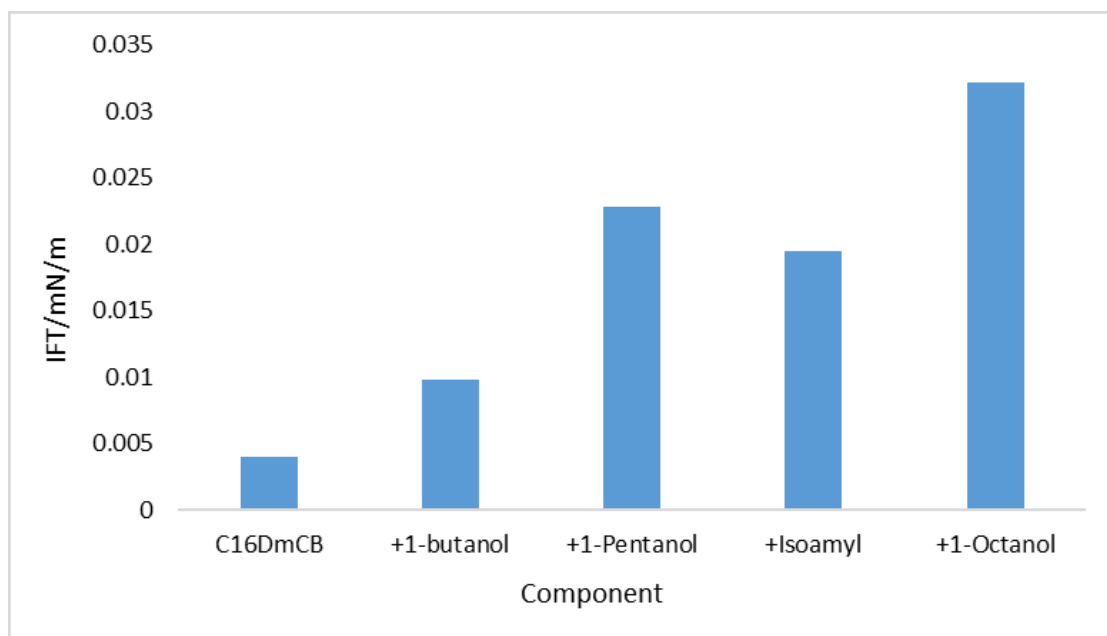
Figure 4. 5 Effect of the addition of small n-alcohols to $C_{16}DmCB$ on IFT

Chapter 5: Zeta Potential Test

In the previous chapter, IFT of different surfactants and surfactant-alcohol systems were studied. In addition to IFT reduction, wettability alteration is also crucial for enhanced microscopic oil recovery, especially in the tight formation. In this chapter, wettability alteration potential of surfactant and surfactant-alcohol systems are studied through zeta potential measurements.

5.1 Methodology

In this study, zeta potential measurements were conducted to evaluate the wettability alteration potential for both the brine/rock and brine/oil systems. Based on the IFT results reported in the previous chapter, the optimal concentration for C_{12}DmCB, C_{14}DmCB, and C_{16}DmCB are 0.25 wt%, 0.025 wt%, and 0.025 wt% respectively. The simulated formation brine was prepared at the salinity of 5k, 10k, 25k, 50k, 100k, 200k ppm separately.

For the case of brine/rock system, Indiana limestone and tight carbonates were crushed into fine particles and 1wt% was used as a suspension in 10ml brine solution. Surfactants at the optimal concentrations mentioned above were initially added to the solutions and a blank controller was also prepared without surfactants. Higher surfactant concentrations (C_{12}DmCB, 0.5wt%; C_{14}DmCB, 0.5wt%; C_{16}DmCB, 0.5wt%) were also tested for potential in altering the wettability. Two surfactants capable of altering the wettability significantly were chosen for studying the effect of co-solvent additions. 1-butanol, 1-pentanol, isoamyl and 1-octanol were the co-solvents used. The surfactant-to-alcohol ratio of 1/6 to 1/2 was used by previous researchers (Okamoto ey al., 2016; Sakamoto et al., 2017) to study the surfactant-alcohol system. In this study, a surfactant-to-alcohol ratio of 1/3.24 was used. The simulated formation water (SFW) was prepared at a wide range of salinities from 5,000 ppm to 200,000 ppm. The surfactant, alcohol and crushed rock

samples were mixed using ultrasonic sonicator. The mixing was done for 30 seconds. The samples were then stabilized for 3 hours at ambient conditions before use.

For the case of brine/oil system, 2ml oil and 10ml brine were mixed together with surfactants at various concentrations (C_{12}DmCB, 0.25wt%; C_{14}DmCB, 0.025wt%; C_{16}DmCB, 0.025wt%). The mixtures were left in a sonicator bath for 20 minutes for better blending and then allowed to rest for one day before use. The same type and concentration of the co-solvents were added to the surfactant solutions compared with the brine/rock system.

Zeta potential of these systems was measured by Zetasizer Nano-ZSP (Malvern Instruments) at ambient temperature. Figure.5.1 describes a schematic of the experimental setup for operation and the apparatus used in this section.
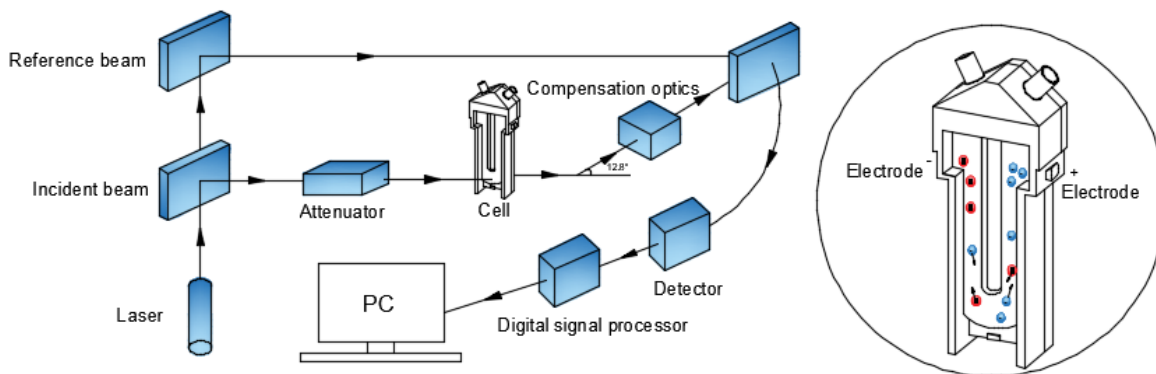
(a)

(b)

Figure 5. 1 (a) Schematic of the experimental setup for the operation of zeta potential measurement; (b) Zetasizer Nano-ZSP

Surfactant solutions were injected into the cell manually. The detailed operation process is as follows.

1. Prepare 0.75ml sample in a syringe and remove the bubbles inside.

2. Invert the cell and place the syringe into one of the sample ports.

3. Slowly inject the sample and fill the U-tube to just over half a way.

4. Turn the cell upright and continue injecting until reaching fill area before the maximum limit line.

5. Tap the tube gently if air bubbles are observed in the cell.

6. Fit the stoppers before measurements and make sure one stopper is fitted firmly and the other one is fitted loosely.

7. Place the cell into the apparatus and start the measurement. One measurement took 100 times, and the final result was the average of six measurements.

Electrophoretic mobility was then measured by the apparatus with conversion to zeta potential inferred from the Helmholtz-Smoluchowski equation, Eq.(19). Where, ζ is zeta potential, U_E is electrophoretic mobility of carbonate particles or oil droplets dispersed in brine, η is liquid viscosity, ε is dielectric constant, $F(\kappa a)$ is Henry's function among which the particle radius is denoted by a, while $1/\kappa$ represents the thickness of the double layer. Thus, κa signifies the ratio of the particle radius to double layer thickness. It has a maximum value of 1.5 (Smoluchowski approximation) for polar media and a minimum value of 1 (Hückel approximation) for non-polar media separately.

$$\zeta = \frac{3U_E\eta}{2\varepsilon F(\kappa a)} \qquad \text{Eq.(19)}$$

5.2 Results and Analysis

5.2.1 Limestone reservoir

Charges at the rock surface and brine/oil interface are responsible for the stability of water film surrounding the rock. Cation exchange and expansion of the electric double layer (EDL) can be the primary mechanisms that give rise to the wettability alteration (Ligthelm et al., 2009; Sandengen et al., 2011), which is indicated by the sign and magnitude of zeta potential.

Figure.5.2 depicts the zeta potential of oil droplets in simulation formation water (SFW) and various surfactant solutions. Results show that the zeta potential remains negative in SFW over the salinity range covered, while the absolute values decrease with the increasing salinity. The zeta potential is strongly sensitive at low salinities of 5,000 ppm and 10,000 ppm with the presence of surfactants, especially for $C_{12}DmCB$ and $C_{14}DmCB$. The dramatic decrease from -17.5 mV to -1.36 mV in magnitude implies the compress of EDL as an adverse impact. The addition of surfactants has minimal effect on the zeta potential values at 25,000 ppm and 50,000 ppm. However, higher magnitude or charge conversion is observed over the high salinity of 100,000 ppm to 200,000 ppm. Overall, the magnitude of zeta potential is highest around 25,000 ppm for all the surfactants studied here irrespective of chain length, however, the absolute values decrease gradually with increase or decrease of salinity from 25,000 ppm.

Indiana limestone composed of calcite is sensitive to the concentration of the brine solution (Figure.5.3). The change of zeta potential with salinity is more pronounced, with a negative value around -4.58 mV at 5,000 ppm up to 10,000 ppm. Beyond 10,000 ppm, zeta potential becomes positive, +10.4 mV at 25,000 ppm. A large portion of divalent cations due to the presence of $CaCl_2 \cdot 2H_2O$ and $MgCl_2 \cdot 6H_2O$ in the SFW result in the more positive value of zeta potential as

salinity increases. The increasing Ca^{2+} and Mg^{2+} absorb to the crushed rock samples continuously and compress the EDL. Thus, an increase in zeta potential dominates the charge conversion. This is consistent with previous studies indicating the addition of polyvalent cations reduces the absolute value of negative charge and conclusively makes it positive (Chen et al., 2014). We can observe that the systems, brine/oil and brine/rock, both are negatively charged at low salinities of 5,000 ppm and 10,000 ppm (Figure 5.2 and figure 5.3). The ions at the rock surface and the ions presented in the brine tend to repel each other, contributing to the EDL expansion. Therefore, water-wet condition is observed. The additive surfactants to the SFW does not have significant effects on the zeta potential of limestone surface over the salinity range mentioned above. When changing over to 25,000 ppm, attractive forces exceed the repulsion as opposite charges are shown in the two systems (Figure 5.2 and figure 5.3), clearly indicating the oil-wet condition. However, zeta potential of the rock surface can change from positive to negative with the presence of surfactants at the salinity range from 25,000 ppm to 100,000 ppm. This is important because the brine/oil system is already negative in the same salinity range (Figure 5.2). EDL expansion and the establishment of the stable water film occur in the whole brine/oil/rock system. Hence, the rock tends to become less oil-wet or completely water-wet which may increase the residual oil recovery during EOR processes. $C_{14}DmCB$ can effectively change the zeta potential from +10.4 mV to -8.42 mV, which gives the highest wettability alteration potential in terms of charge conversion and higher magnitude of zeta potential (Figure 5.3). At 200,000 ppm, the surfactant addition to the SFW does not change the surface charge of limestone from positive to negative. However, the additives change the zeta potential of oil droplets from the negative to positive. Thus, it ends up having two systems (Figure 5.2 and Figure 5.3) with positive charges that could repel each other. Therefore, wettability of the whole brine/oil/rock system changes from oil-wet to water-wet.

However, the extent to which wettability alteration occurs at 200,000 ppm salinity is less when compared to the 25,000 ppm and 100,000 ppm. Higher magnitude of zeta potential values that presented due to surfactant addition in the salinity range from 25000 ppm to 100,000 ppm could be the attributed reason.
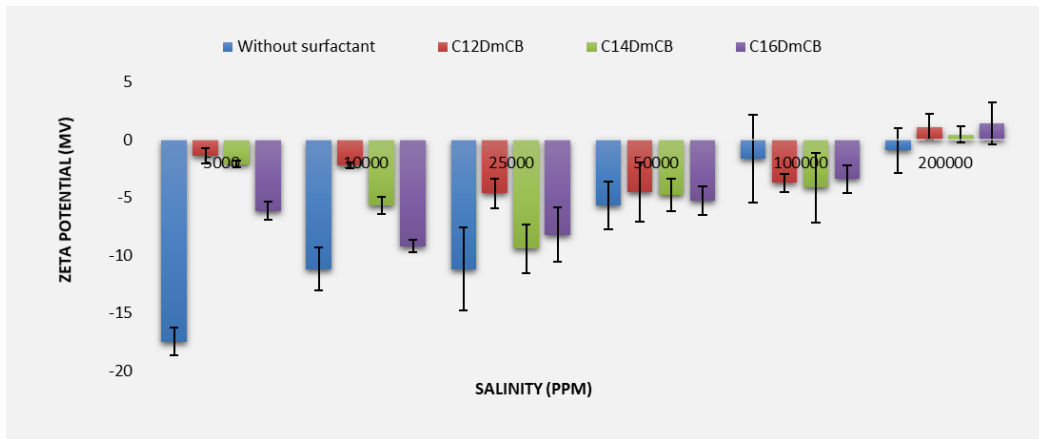
Figure 5. 2 Zeta potential of oil droplets in SFW and various C_nDmCB surfactant solutions
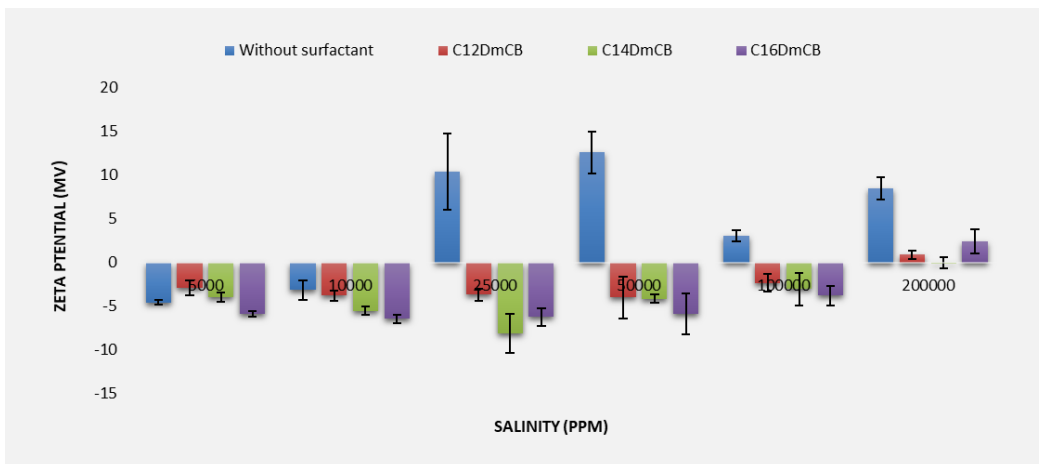
Figure 5. 3 Zeta potential of limestone particles in SFW and various C_nDmCB surfactant solutions

The pH of the solutions is given in Figure.5.4. The pH of the SFW increases with the reduction of salinity. Higher pH values correspond to more hydroxyl groups in the solution. Thus, more negative charges are added to the limestone surface, resulting in the negative zeta potential at the low salinity of 5,000 ppm and 10,000 ppm. A similar trend of reduction and a higher level

of pH values are found by adding surfactants, especially for the presence of $C_{14}DmCB$ and $C_{16}DmCB$ in comparison to $C_{12}DmCB$. Moreover, the effect of higher surfactant concentration on the zeta potential of the limestone surface is also taken into consideration (Figure 5.5). A slight decrease in the absolute value of zeta potential is observed, indicating an adverse effect with increasing surfactant concentration.

Figure 5. 4 The pH of the brine/limestone system with salinity in SFW and various C_nDmCB surfactant solutions
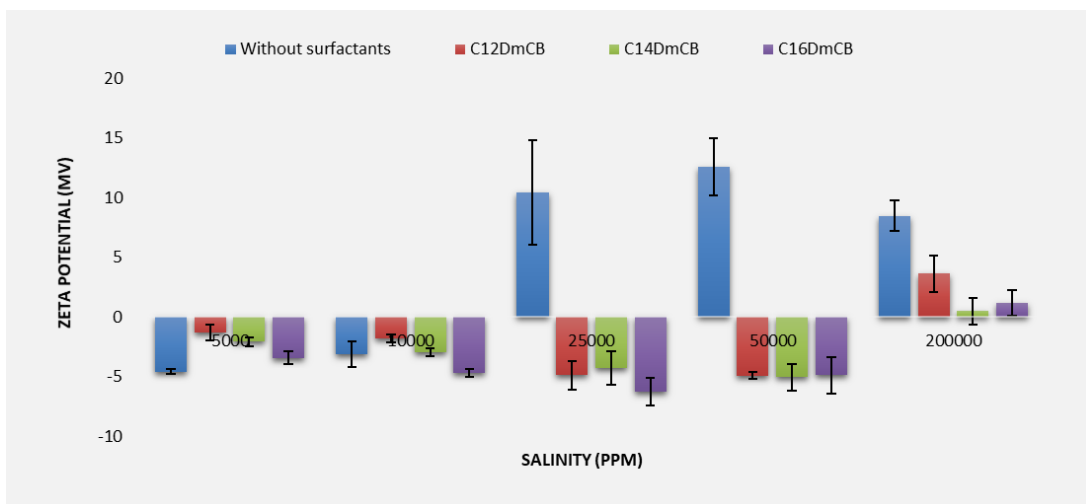
Figure 5. 5 Zeta potential of limestone particles in SFW and various C_nDmCB surfactant solutions at higher surfactant concentrations

The effect of the additive alcohols with different carbon chain lengths and structures to $C_{14}DmCB$ on the brine/oil system is shown in Figure.5.6. At low salinity of 5,000 ppm, the addition of alcohols increases the magnitude of zeta potential while it remains relatively stable as the salt concentration increases until 200,000 ppm where the magnitude increases again. Among different types of alcohols, it is inferred that the absolute value of surfactant/alcohol formulation with the presence of 1-butanol is the highest in an extensive range of salinity. The magnitude of zeta potential tends to get lowered with the increasing carbon chain length of the alcohols. 1-pentanol and isoamyl alcohol have similar alkyl chain length but different structures. However, isoamyl alcohol addition to the surfactant results in the higher magnitude of zeta potential values and charge reversal. Therefore, it can be said that isoamyl alcohol characterized by additional CH_3 group could be a better additive to the studied zwitterionic surfactant.
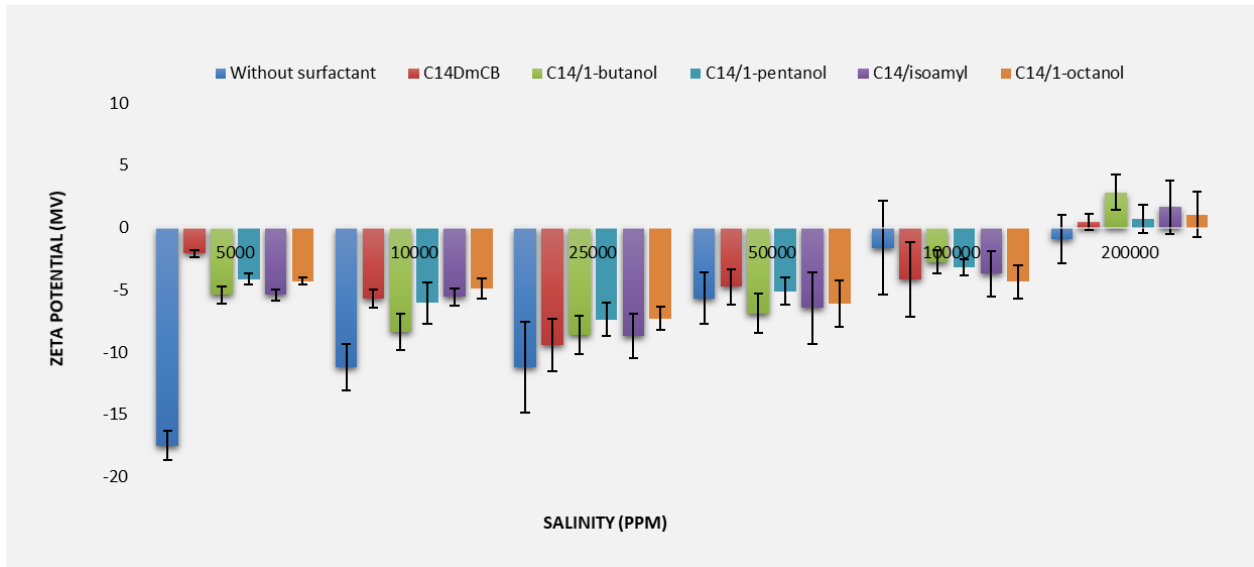
Figure 5. 6 Effect of additive alcohols to $C_{14}DmCB$ on the zeta potential of oil droplets in SFW and various surfactant solutions

The impact of adding 1-butanol, 1-pentanol, isoamyl, and 1-octanol to $C_{14}DmCB$ for the brine/rock system was studied and shown in Figure 5.7. The addition of alcohols further increases the magnitude of zeta potential of the surfactant at the low salinity of 5,000 and 10,000 ppm,

leading to the expansion of the EDL and enhancing the repulsion force. Among the four different alcohols that were added to surfactant, 1-butanol shows the higher wettability alteration potential at the salinity of 5,000 ppm and 100,000 ppm. Increasing the salinity to 25,000 ppm results in the diminished magnitude of zeta potential for all the four surfactant-alcohol systems. Increasing the salinity to a higher level does not improve the wettability alteration potential of alcohol additions to the surfactant. Usually, the magnitude of zeta potential in the range of 30 mV/m is considered to be the threshold value that corresponds to good electric stability.
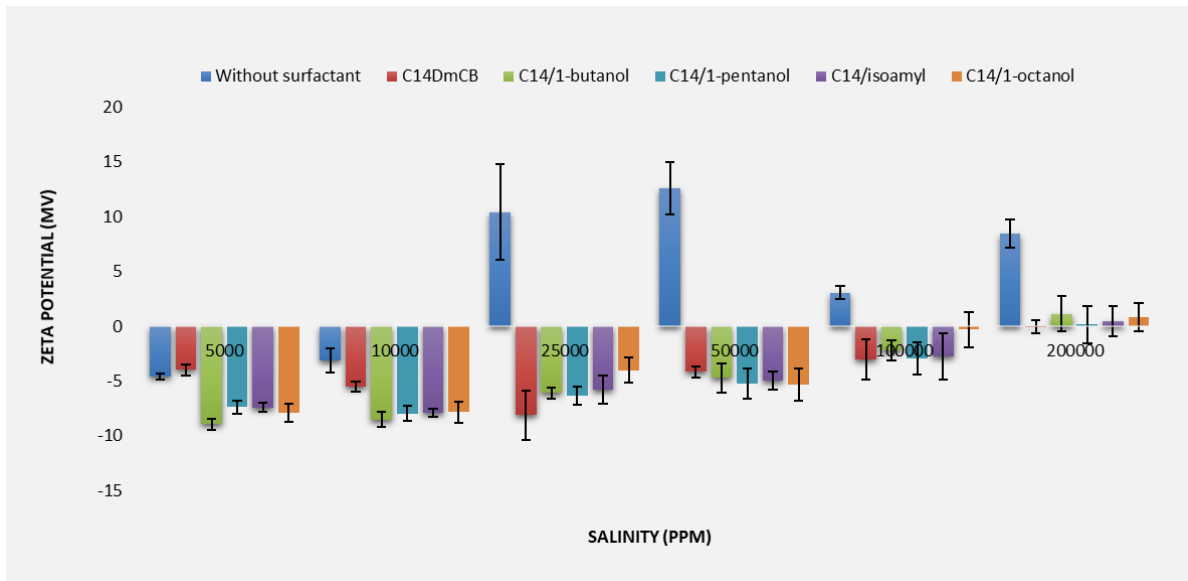
Figure 5. 7 Effect of additive alcohols to $C_{14}DmCB$ on the zeta potential of limestone surface in SFW and various surfactant solutions

The pH of the surfactant solution decreases with the presence of alcohol additions (Figure.5.8). As the salinity increases, pH values of all the surfactant/alcohol systems become progressively lower. However, all the four alcohols have a similar effect in terms of pH reduction on the surfactant over the salinity range studied.
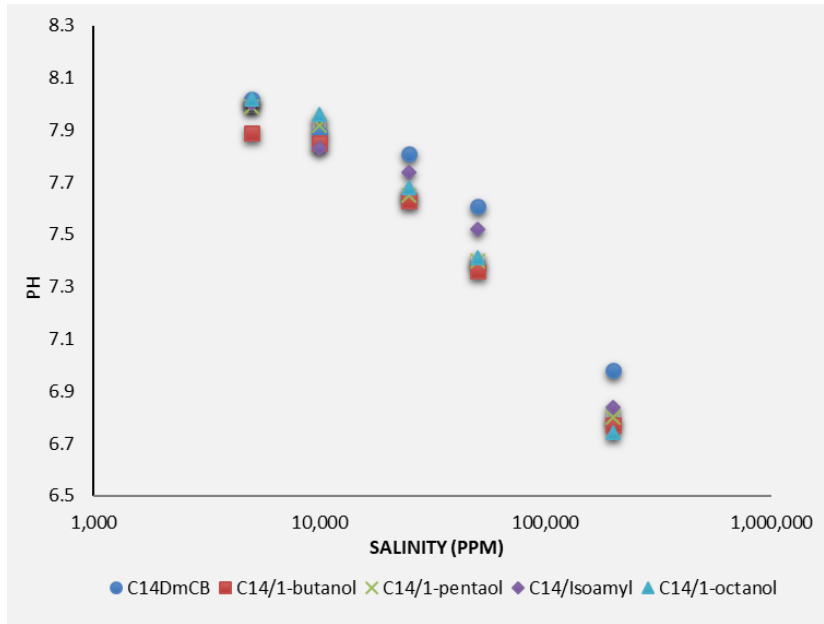
Figure 5. 8 The pH of the brine/limestone system with salinity in $C_{14}DmCB$ solution and $C_{14}DmCB$/alcohol formulations

For comparison, the zeta potential of limestone surface and oil droplets in SFW, $C_{16}DmCB$ solution, and $C_{16}DmCB$/1-butanol solution is shown in Figure.5.9 and Figure.5.10. A similar effect of surfactant and alcohol addition to surfactant is observed.
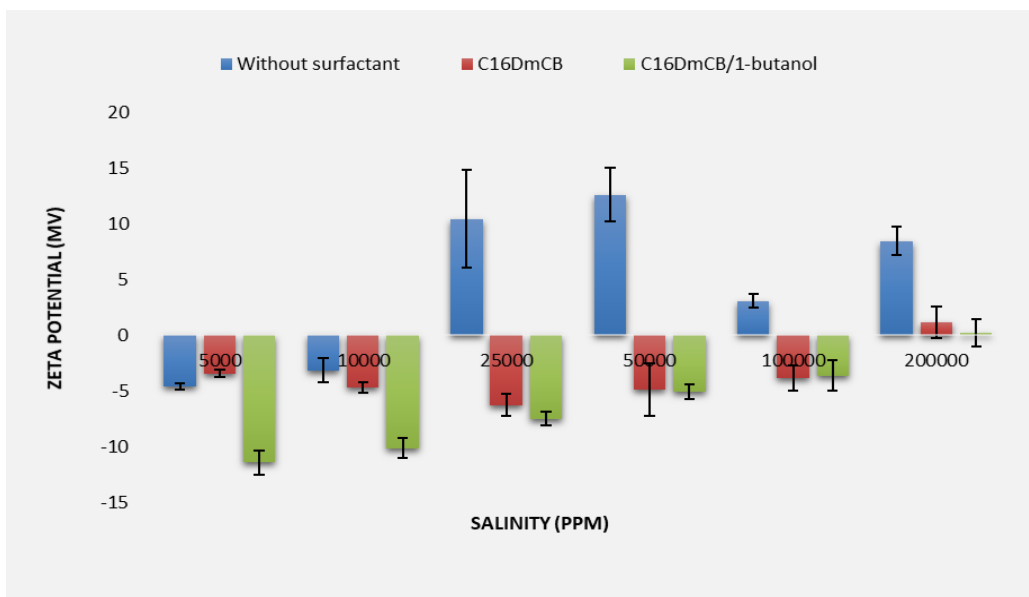
Figure 5. 9 Zeta potential of limestone surface in SFW, $C_{16}DmCB$, and $C_{16}DmCB$/1-butanol solution with salinity
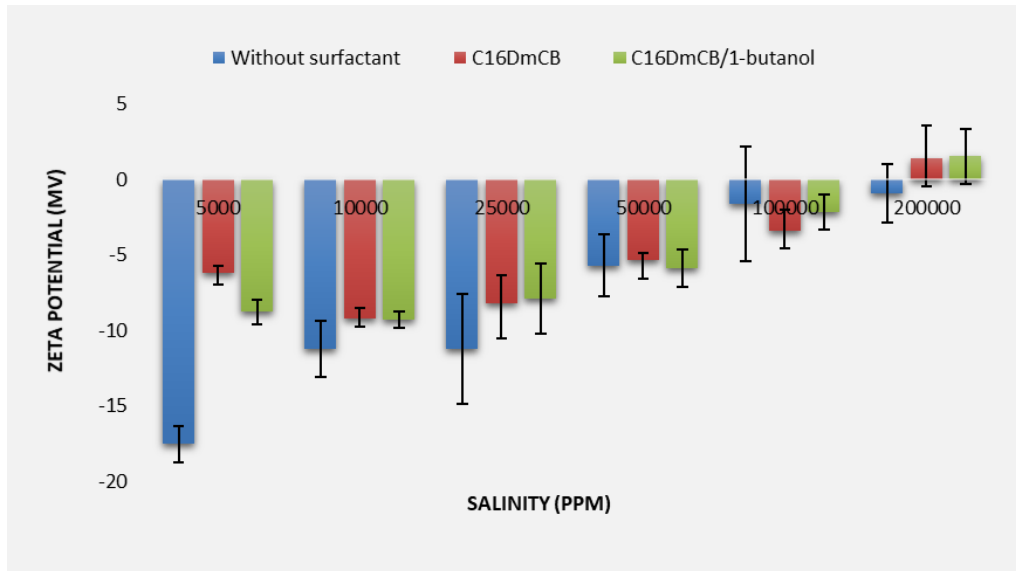
Figure 5. 10 Zeta potential of oil droplets in SFW, C16DmCB, and C16DmCB/1-butanol solution with salinity

From above, we can conclude that charge conversion of zeta potential dominates the wettability alteration potential. Like charges repel each other, contributing to the expansion of the EDL. The addition of surfactants and co-solvents reacts differently at varying salinities. Additive surfactants have negative or minimal impact at the low salinity of 5,000 ppm and 100,000 ppm. However, the absolute value can be improved by adding alcohol-based co-solvents. $C_{14}DmCB$ can effectively change the wettability of the limestone surface from oil-wet to water-wet at 25,000 ppm.

5.2.2 Tight carbonate reservoir

Tight carbonate reservoirs possess ultra-low permeability and large pressure gradient. Figure 5.11 depicts the Scanning Electron Microscope (SEM) micrography and Energy-Dispersive X-ray (EDX) for the tight carbonate sample we studied. Results show that the rock sample consists of calcium and magnesium ions, which are different than that of limestone components.

(a)

(b)

67

Element	Weight%	Atomic%
O K	58.43	74.92
Mg K	12.62	10.65
Ca K	26.25	13.44
Fe K	2.69	0.99
Totals	100	
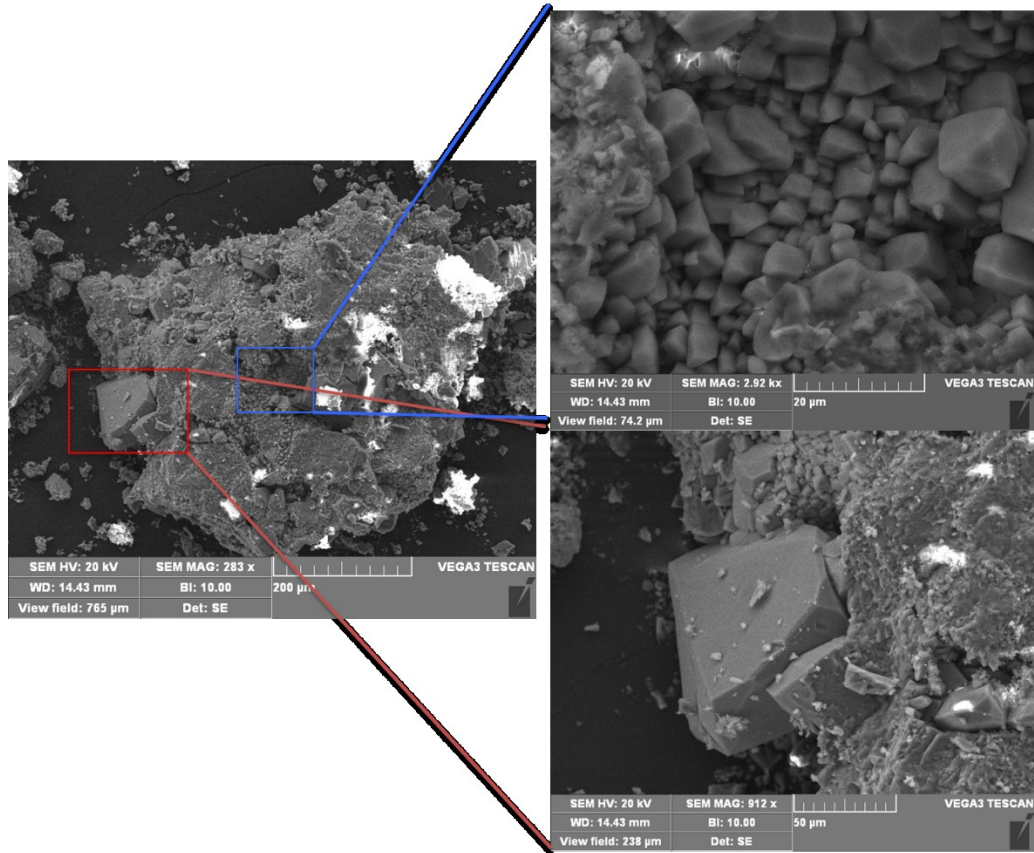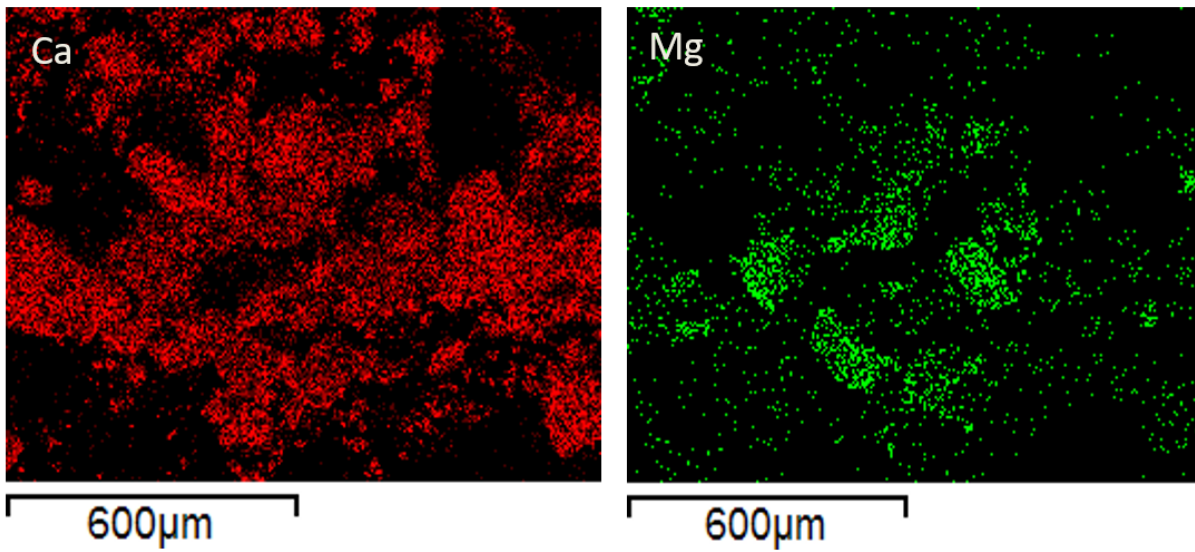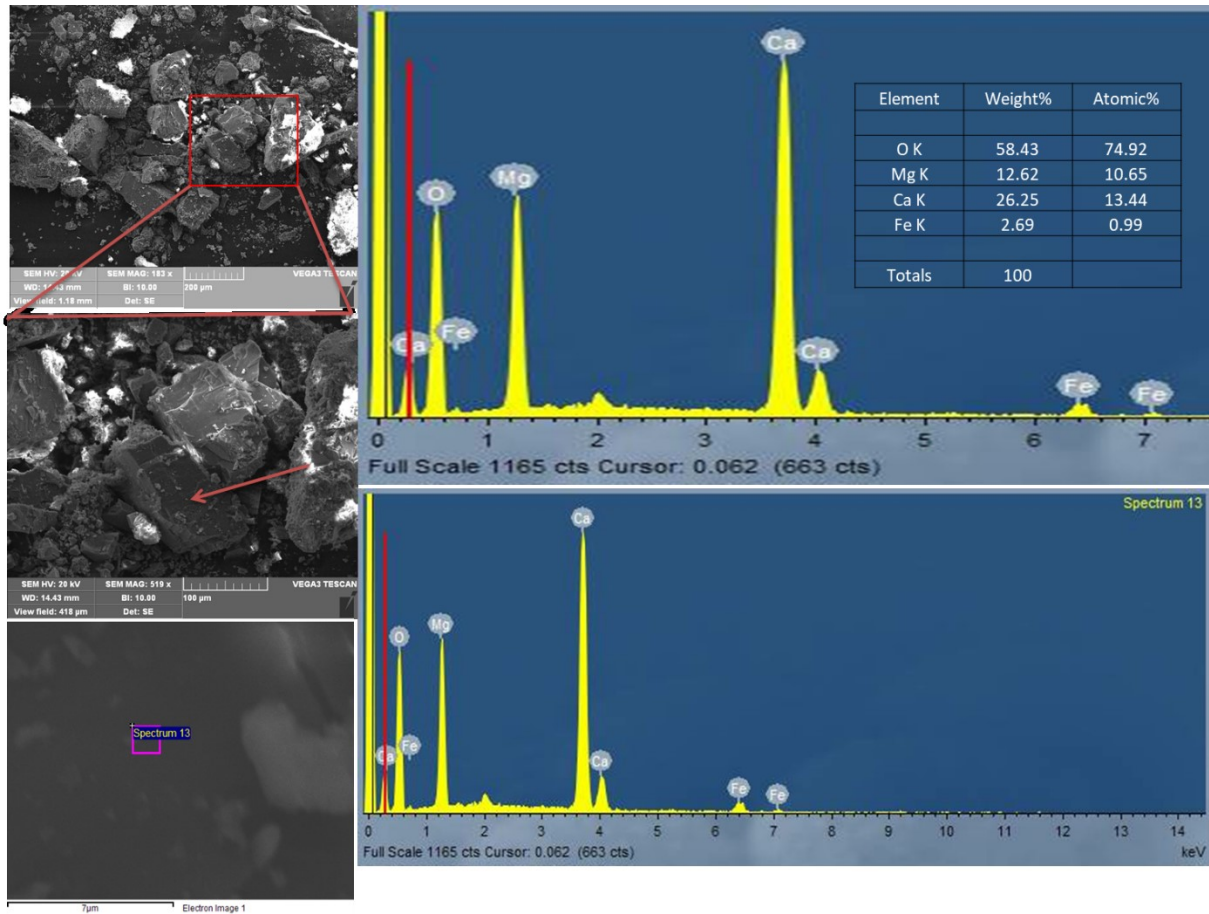
(c)

Figure 5. 11 (a) SEM micrography for tight carbonate reservoir; (b) Elemental mapping; (c) EDX spectra for tight carbonate reservoir

Figure 5.12 shows the impact of different formulations of alcohol-surfactant systems on zeta potential of the brine/rock system. Different from limestone rock, the surface charges of tight carbonate rock are all positive over an extensive range of salinities from 5,000 ppm to 200,000 ppm. This is due to the existence of magnesium ions in the rock samples, giving more positive charges at the rock surface. The addition of surfactants efficiently changes the charges from positive to negative. The same polarity with the brine/oil system is observed, elucidating the expansion of the EDL. The magnitude of zeta potential of surfactant becomes more substantial at all the salinities from 5,000 ppm to 200,000 ppm with the increasing carbon chain length, resulting

68

in more prominent repulsion force and hence a possibility for higher oil recovery. However, the reduction of magnitude in zeta potential is observed for every surfactant as the salinity increases. The influence of adding 1-butanol to surfactant is not significant in tight carbonate when compared to limestone rock. Thus, we can conclude that alcohols have different effects on the reservoirs based on their petrophysical properties or original status. Overall, surfactant $C_{16}DmCB$ is recommended for tight carbonate reservoirs for a wide range of salinities from 5,000 ppm to 200,000 ppm
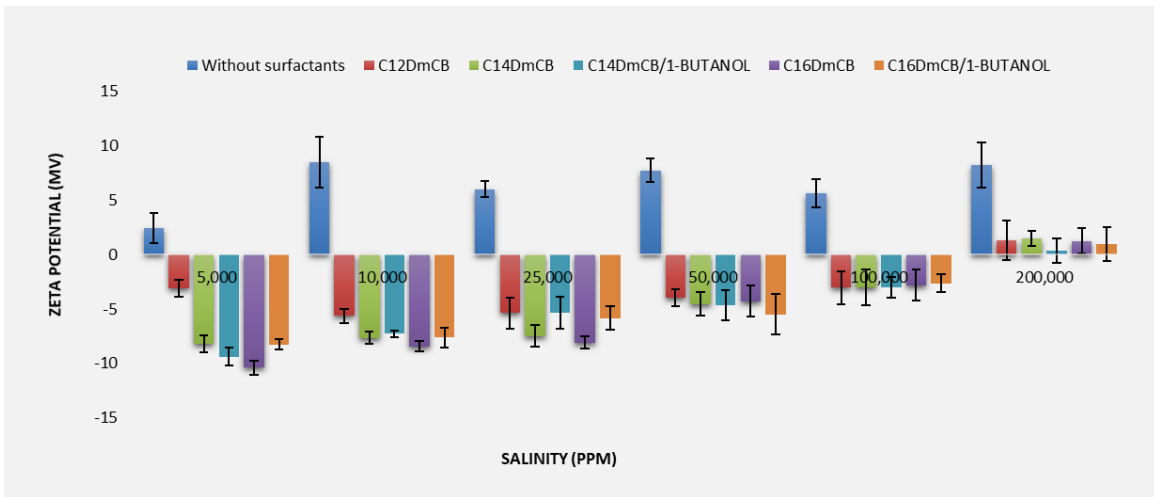
Figure 5. 12 Effect of diverse additions on the brine/tight carbonate#1 system
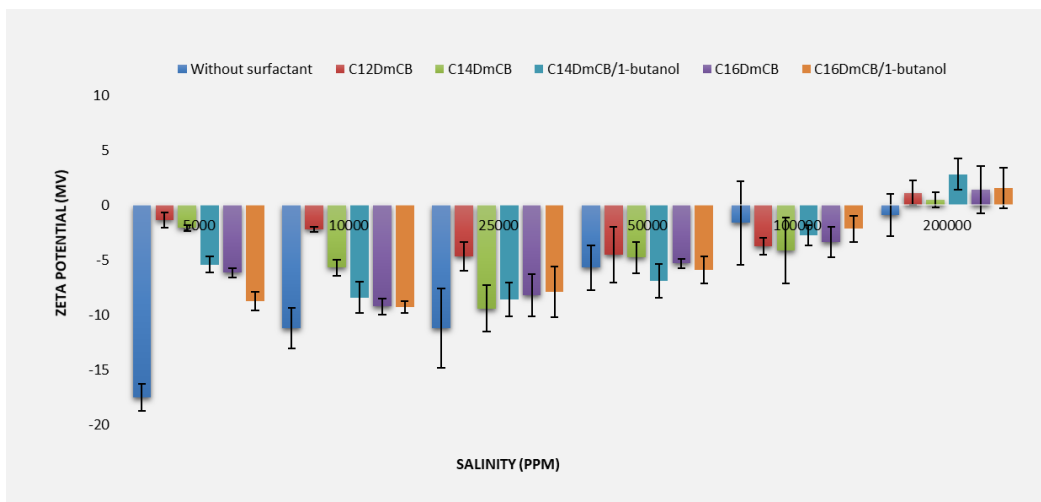
Figure 5. 13 Effect of diverse additions on the brine/oil system

The tight carbonate rock from another well at different depth which was similar to that of limestone rock was also used for studying the wettability alteration potential of brine, surfactant/brine and surfactant/brine/cosolvent systems (Figure 5.14). The surface charges of the rock are all positive at varying salinities from 5,000 ppm to 200,000 ppm and the difference of magnitude in zeta potential is not significant. The addition of surfactants changes the surface charges from positive to negative except at the extremely high salinity of 200,000 ppm. It is interesting to see that the highest magnitude is observed at 25,000 ppm which becomes lower as salinity increases or decreases. This phenomenon is the same as what we find in limestone reservoir. However, the influence of alcohols is not apparent even at the low salinity of 5,000 ppm and 10,000 ppm.
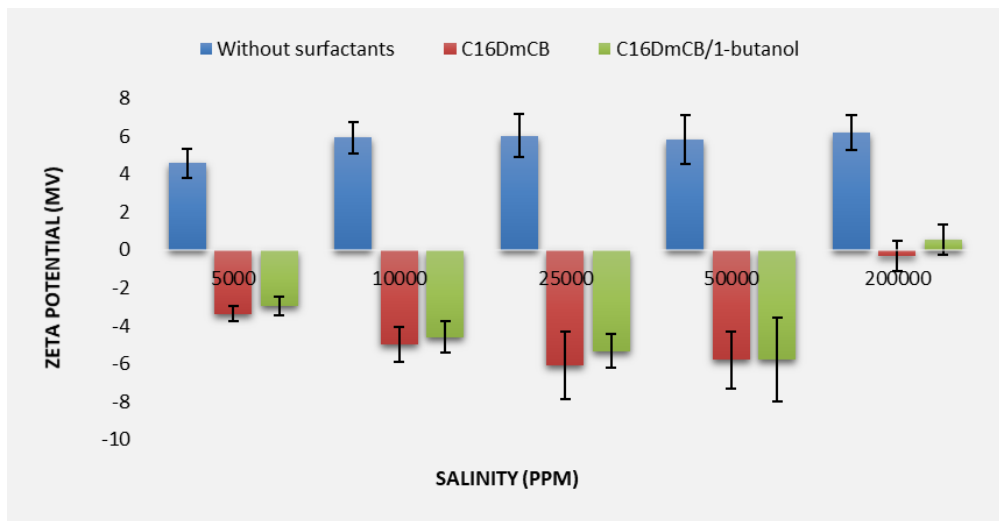
Figure 5. 14 Effect of diverse additions on the brine/tight carbonate#2 system

Chapter 6: Micromodel flood test

In the previous chapters, interfacial properties in terms of IFT and wettability alteration potential in terms of zeta potential test have been studied and analyzed. In this chapter, micromodel flood test was further conducted to understand the dominant mechanism that gives rise to the enhanced oil recovery under high saline conditions. Water-wet and oil-wet porous media were studied separately using different C_nDmCB and C_nDmCB/1-butanol solutions.

6.1 Methodology

The experimental setup of the micromodel flood test mainly includes an injection pump and a micromodel, as shown in Figure 6.1. A non-transparent micromodel made of silicon and glass provided a homogeneous porous media; while a transparent micromodel made of etched glass gave a heterogeneous porous media. In each test, the micromodel was first saturated with reservoir oil at the injection rate of 0.05 ml/min from the right side to the left side until complete saturation. The oil inside the syringe was then expelled out and the syringe was washed with toluene once and deionized water twice. Surfactant solution was further inhaled into the syringe for each test and then injected to the porous media at a low injection rate of 0.1 ml/hour. The oil displacing process was recorded at three different locations with time using a digital camera, especially when the flood front went across the boundary of the micromodel at the early time, when the breakthrough happened, and when significant changes occurred. All the experiments were conducted at ambient conditions with the micromodel placed horizontally to avoid gravity effects.

Figure 6. 1 The experimental setup of the micromodel flood test

In this work, micromodel flood test was conducted with different surfactant formulations based on the analysis of the physicochemical interaction in both water-wet and oil-wet porous media. Table 6.1 shows the components of different formulations used in this section along with the corresponding IFT characteristics and wettability alteration properties. The formulation (0.025wt% C_{16}DmCB, 100k ppm) that generated the ultralow IFT, referred as F1, was injected to the water-wet and oil-wet homogenous micromodel. Effect of the 1-butanol as co-solvent on F1 surfactant formulation, referred as F2, for oil displacement pattern was further studied. F1 results in the lowest IFT at high salinity but is ineffective for wettability alteration, whereas F2 has higher IFT compared to F1 and has a poor potential to alter the wettability. Thus, F2 was only studied under the water-wet condition. In another set of experiments, C_{16}DmCB and C_{14}DmCB surfactant solutions in low salinity brine of 25,000 ppm, referred as F3 and F4 respectively, were injected into both the water-wet and oil-wet homogeneous micromodel to understand the effect of surfactant type effect. Moreover, the comparison of F1 and F3 flooding experiment will explain

the effect of salinity on $C_{16}DmCB$ surfactant. It is important to note that F1 formulation has lower IFT ($4.81*10^{-3}$ mN/m) than F3 formulation ($6.6*10^{-3}$ mN/m mN/m). The zeta potential of limestone particles changes from +10.4 mV to -8.12 mV with the presence of F4; however, it only changes from +3.07 mV to -3.79 mV by the addition of F1. Hence, F3 formulation has higher potential to alter wettability than F1 due to higher magnitude of the change of zeta potential in the brine/rock system. Similar is true between F1 and F4 formulations (Table 6.1). Therefore, comparing oil displacement mechanism between F1 and F3 as well as F1 and F4 will able to answer the dominating mechanism between IFT reduction and wettability. In summary, four formulations including F1 to F4 were studied in the water-wet homogeneous porous media, whereas only F1, F3 and F4 were studied in the oil-wet one. In a final micromodel flood, two different surfactants were injection in series one after another. A Nonyl-phenol-ethoxylate (non-ionic surfactant) surfactant with 1 wt% in 100,000 ppm salinity (F5), having a strong potential for altering wettability, was injected followed by 0.025wt% $C_{16}DmCB$ surfactant solution (F1) with ultralow IFT.

Table 6. 1 Different surfactant formulations injected into the micromodel

No.	Surfactant formulation	Surfactant concentration	Salinity	IFT (mN/m)	Wettability alteration
F1	$C_{16}DmCB$	0.025wt%	100k ppm	$4.81*10^{-3}$/ Excellent	Poor
F2	$C_{16}DmCB$/1-butanol	0.025wt%	100k ppm	$9.8*10^{-3}$/ Good	Poor
F3	$C_{16}DmCB$	0.025wt%	25k ppm	$6.6*10^{-3}$/ Good	Excellent
F4	$C_{14}DmCB$	0.025wt%	25k ppm	0.115/ Poor	Excellent
F5	Nonyl-phenol-ethoxylate nonionic surfactant	1wt%	100k ppm	0.24/ Poor	Excellent

To change the wettability of micromodel, which was initially water-wet, two procedures were followed including the chemical conversion and experimental verification in terms of contact angle measurement. 10 vol% siloxane was mixed with 90 vol% pentanol and injected into the clean chip. Pentanol and methanol were then injected separately to remove the excess chemicals from the pore structures. The micromodel was dried in the oven for 1 hour and then dried at the ambient condition for 24 hours before use. To verify the wettability conversion of the micromodel, the glass material was treated the same way and confirmed by the contact angle test. Both the untreated and treated glass were immersed in DI water separately. An oil droplet was then injected to the glass surface to evaluate the wettability condition. Results show that the contact angle of the oil droplet changes from 89° to 40° after being treated with the chemicals (Figure 6.2), which means the glass has been changed successfully into the oil-wet. Moreover, the wettability alteration potential of F1 and F4 formulations were tested on the same glass surface using contact angle test to verify the zeta potential results. An oil droplet was injected to the glass surface immersed by either F1 or F4. The contact angle between the oil and surfactant solution was then measured.

(a)   (b)
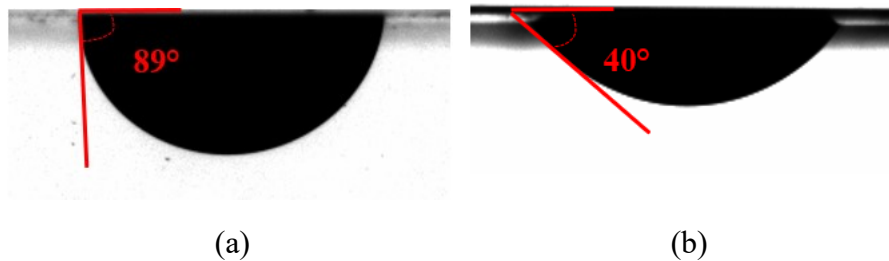
Figure 6. 2 Oil droplet on the glass surface immersed in water (a) before and (b) after being treated with the chemicals

6.2 Results and Analysis

Figure 6.3a depicts the initial status of the water-wet homogenous chip. The reservoir oil fills the pores gradually as the injection takes place (Figure 6.3b) until full saturation (Figure 6.3c).
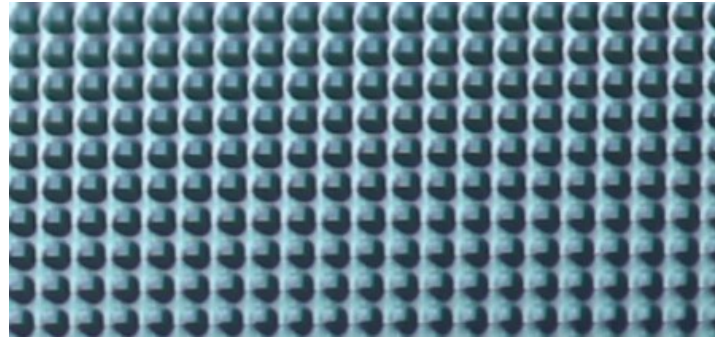
(a)
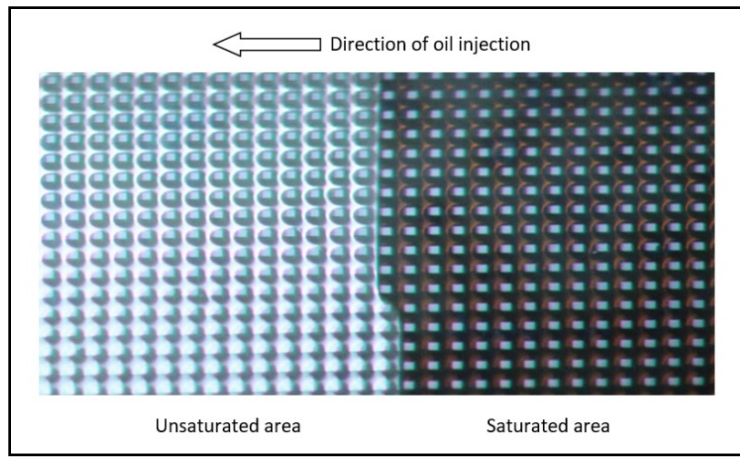
(b)
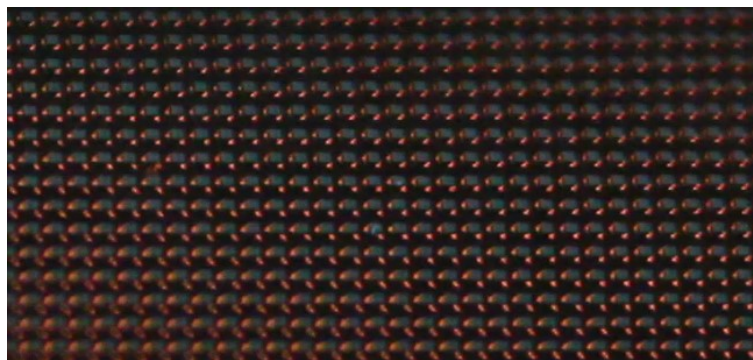
(c)

Figure 6. 3 Oil saturation process from the original status to the final status of the water-wet homogenous chip (a) Original status of the homogeneous chip; (b) Oil injection from right to left; (c) Full oil-saturated status of the homogenous chip

Figure 6.4 shows the oil displacement pattern in the water-wet homogeneous porous media with the injection of F1 to F4 at three locations during different stages. As can be seen from the Figure
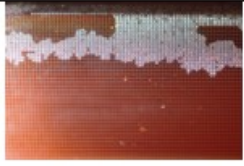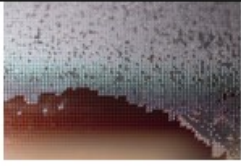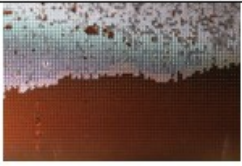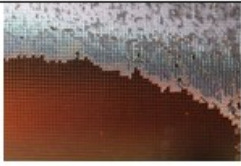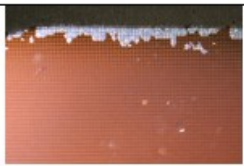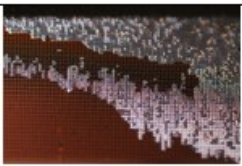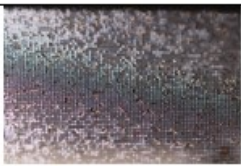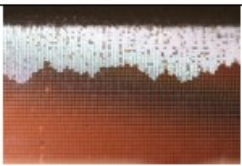
6.4a, the injection of F1 and F2 result in higher displacement efficiency at the early stage and the breakthrough takes place earlier than that of the lower-salinity solutions (F3, F4). The fingering phenomenon is more obvious with the presence of higher-salinity formulations. Since the IFT of F1 and F2 is lower in comparison to F3 and F4, the relative movement of surfactant solution through oil-saturated micromodel is faster. Besides, both F1 and F2 can give excellent oil recovery as most of the oil is expelled out of the micromodel after 5-hour injection (Figure 6.4e). Thus, there exists a correction between lower IFT and higher oil recovery with the presence of surfactant solutions in the studied water-wet homogeneous porous media. The effect of additive 1-butanol to F1 does not have significant effect during the whole injection process. However, different flow patterns are shown between F2 and F3 that have similar IFT results. Pei et al. (2014) reported that the reduction of viscosity of microemulsion resulted in a more movable fluid by adding alcohols to alkali solution. Thus, higher displacement efficiency and tertiary oil recovery are observed. Redistribution of oil pattern is found after breakthrough due to the boundary effect. After long-time injection of surfactant solutions, there is still a small amount of residual oil trapped in the pores (Figure 6.5).

9'11''	LOCATION 3	LOCATION 2	LOCATION 1
F1			
F2			
F3			(5'00'') (9'11'')
F4			
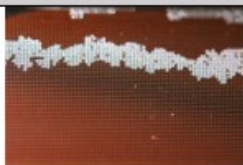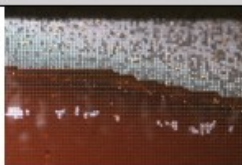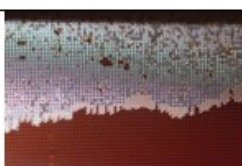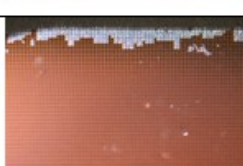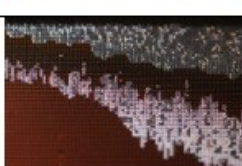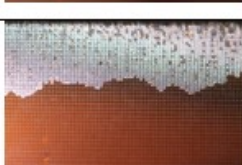
(a)

19'30''	LOCATION 3	LOCATION 2	LOCATION 1
F1			
F2			
F3			
F4			

(b)

78
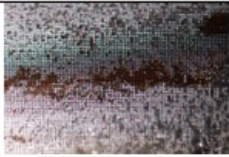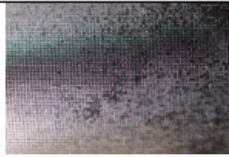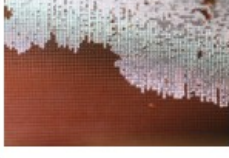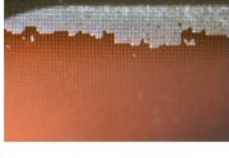
40'00''	LOCATION 3	LOCATION 2	LOCATION 1
F1			
F2			
F3			
F4			

(c)

1HR	LOCATION 3	LOCATION 2	LOCATION 1
F1			
F2			
F3			
F4			

(d)

5HRS	LOCATION 3	LOCATION 2	LOCATION 1
F1			
F2			
F3			
F4			

(e)

Figure 6. 4 Oil displacement pattern in the water-wet homogeneous porous media with the injection of F1-F4 during different stages (a) 9'11''; (b) 19'30''; (c) 40'00''; (d) 1 hour; (e)5 hours

Figure 6. 5 Residual oil trapped in the water-wet pore structures

In the oil-wet porous media, wettability alteration potential needs to be taken into consideration. Results show that the contact angle changes from 40° to 95° in F1 solution indicating that the oil-wet condition is changed to mixed-wet (Figure 6.6a). Furthermore, the

wettability of the glass surface can be changed to completely water-wet in F4 solution since the contact angle changes from 40° to 122° (Figure 6.6b). Similar to the results obtained from zeta potential test, F4 has higher wettability alteration potential than that of F1.
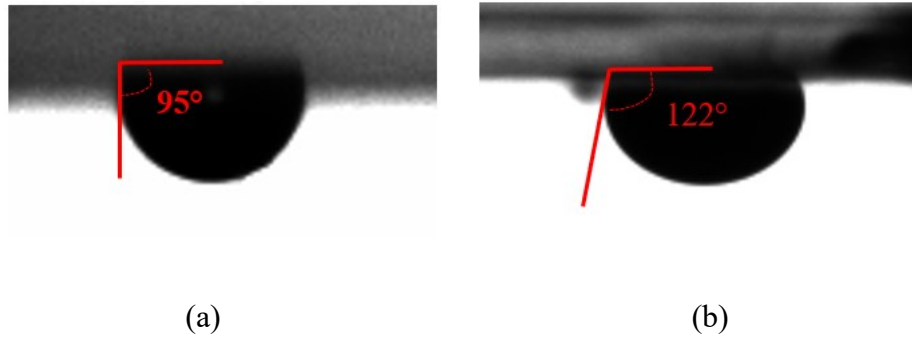

<div align="center">(a)   (b)</div>
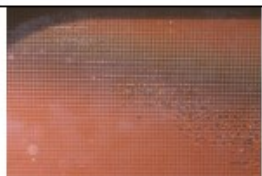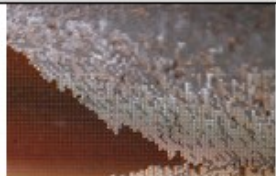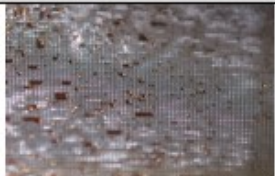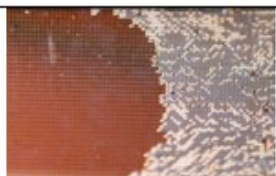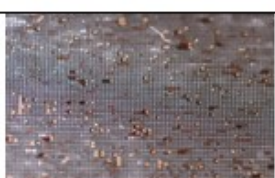
Figure 6. 6 Oil droplet on the glass surface immersed in (a) F1 formulation and (b) F4 formulation

Figure 6.7 shows oil displacement phenomena in oil-wet micromodel for the formulations F1, F3 and F4. The oil displacement pattern in oil-wet porous media is different than that of water-wet pores (Figure 6.4). In the early stage of injection, more time is required for the surfactant solutions to imbibe through the micromodel in comparison to water-wet condition. Compared with F1 that has poor potential for altering wettability, F3 and F4 offer more efficient flooding process in terms of higher oil recovery (Figure 6.7a). The residual oil trapped behind is also lower for F3 and F4 formulations. As studied earlier, F4 can effectively change the wettability of the glass surface from oil-wet to water-wet. Hence, wettability alteration dominates the early stage of oil displacement process, which allows the target solutions to get imbibed into the pores first. However, the displacement efficiency is changed among different formulations and the flooding process lasts shorter during the late time after the oil displacement starts. The injection of F1 gives a faster movement of the flowing fluid and oil in the pores is expelled out earlier than other formulations (Figure 6.7c). Thus, low IFT is necessary for the late time recovery, resulting in the higher ultimate recovery factor. Wettability alteration can only give a quick recovery, but the trapped oil can only

be mobilized if its capillary is reduced which is done by low-IFT agents. The observations are significant to emphasis the importance of ultra-low IFT versus wettability alteration. A small amount of oil is trapped and remained in the micromodel as shown in Fig.6.8.

(a)

(b)

	LOCATION 3	LOCATION 2	LOCATION 1
F1 1hr20'			
F3 1hr40'			
F4 1hr45'			

(c)

Figure 6. 7 Oil displacement pattern in the oil-wet homogeneous porous media with the injection of F1, F3 and F4 during different stages (a) 1 hour; (b) 1 hour 10 min; (c) Final status of the micromodel and the corresponding time taken to reach the final status of the flooding
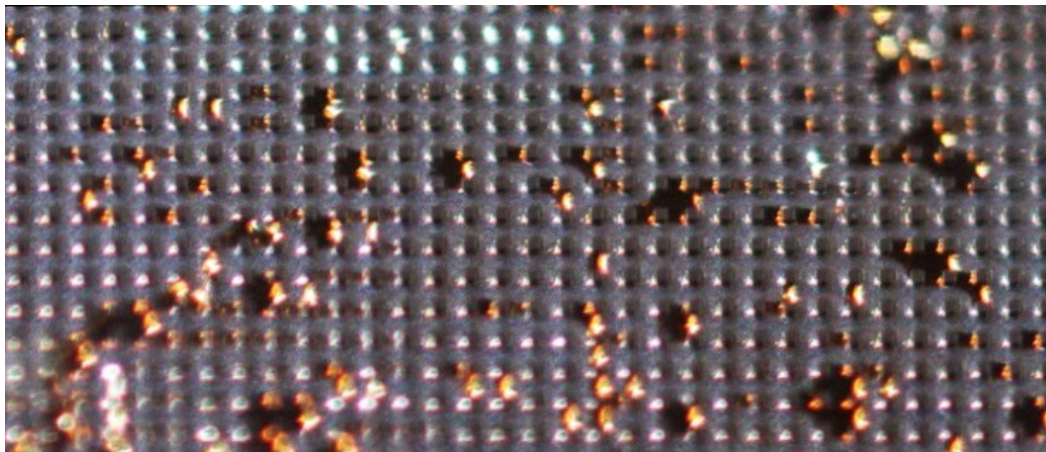
Figure 6. 8 Residual oil trapped in the oil-wet pore structures

Figure.6.9 depicts the oil displacement process in the heterogeneous micromodel by the injection of F5 solution after when F1 solution was injected. The injection is from the right side of figure and the oil displacement follows from right to left. Oil in the fractures can be flushed easily

while it is still trapped in the pores and displaced slowly during injection of F5 (Figure 6.9a-d). After 50-hour injection, F5 surfactant solution can only imbibe into the matrix area near the inlet of injection displacing the oil. However, the injection of the F1 solution highly improves the result in terms of either the displacement efficiency or tertiary oil recovery (Figure 6.9e-g). Most of the oil is displaced after the injection of F1 in the whole studied micromodel (Figure 6.9g). F5 surfactant solution may help in the wettability alteration at the beginning, but IFT reduction caused by the injection of F1 formulation dominates the overall oil recovery process including the ultimate recovery factor.
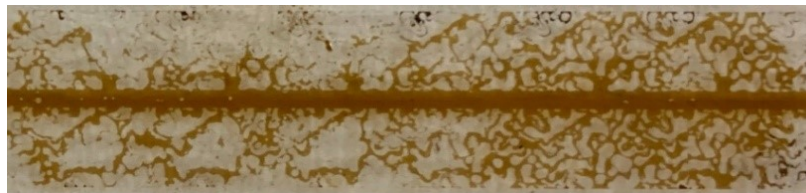
(a)
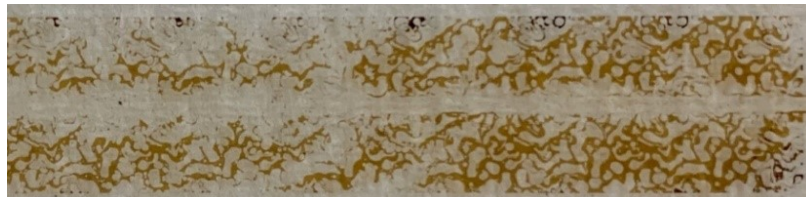
(b)

(c)

(d)

(e)

(f)
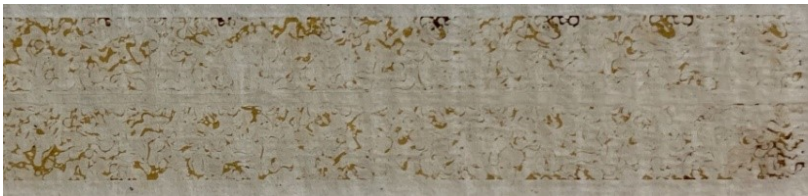
(g)

Figure 6. 9 The oil displacement pattern with the injection of F5 and then F1 in the heterogeneous micromodel (a) Full oil-saturated status; (b) F5 injection after 5 hours; (c) F5 injection after 35 hours; (d) F5 injection after 50 hours; (e) F1 injection after 5 hours; (f) F1 injection after 25 hours; (g) F1 injection after 50 hours

Chapter 7: Conclusions

In tight carbonate reservoirs, wettability alteration and IFT reduction are two main mechanisms that lead to the enhanced oil recovery. The question arises which mechanism dominants the surfactant flooding process. To test this, carboxybetaine based zwitterionic surfactants (C_nDmCB) were chosen for the study due to its ability to reduce IFT to ultralow level at extremely low concentrations and potential to alter the wettability. Experiments in terms of IFT measurements, zeta potential and contact angle test, micromodel flood test were conducted using different C_nDmCB and C_nDmCB/co-solvents with varying salinities from 5,000 ppm to 200,000 ppm. Following conclusions can be drawn:

1. IFT decreases with the increasing carbon chain length except for $C_{18}D_mCB$ due to its poor solubilization in the high saline produced water. The lowest IFT reaches an ultralow level of $4.81*10^{-3}$ mN/m for 0.025 wt% $C_{16}D_mCB$ at 100,000 ppm.

2. IFT decreases first and then increases or remains steady with the increasing surfactant concentration. CMC of $C_{12}DmCB$, $C_{14}DmCB$ and $C_{16}DmCB$ can be inferred from the turning point, which are 0.25wt%, 0.025wt%, 0.025wt% respectively.

3. The addition of alcohol-based co-solvents to C_nDmCB has an adverse effect on IFT due to the increase in IFT. The magnitude differs from the alkyl chain length and the structure of co-solvents. The additive 1-butanol has a minimal negative effect on IFT.

4. The zeta potential of oil droplets is negative over the studied salinity except for 200,000 ppm. The limestone surface is negatively charged at low salinities after which it becomes positive from 25,000ppm. The surface charge of tight carbonate rock is positive overall due to the extra component of magnesium ions. The addition of surfactants changes the opposite charges of the two mentioned systems into the same polarity after 25,000 ppm with limestone particles and tight carbonate samples over the studied salinities, indicating

wettability alteration. 0.025 wt% $C_{14}DmCB$ has a strong potential for altering the wettability at 25,000 ppm.

5. The addition of alcohols to C_nDmCB has different impacts on the potential to alter the wettability in terms of zeta potential. Results differ with the salinity, rock type and alcohol type. The alcohols tend to improve the negative effect caused by the surfactant additions at the low salinity range in the limestone reservoirs. However, the influence in other cases is not apparent.

6. There exists a correlation between lower IFT and higher tertiary oil recovery with the presence of surfactants in the water-wet porous media. The addition of 1-butanol as co-solvent does not have significant effect on the ultimate recovery factor in the surfactant flooding process. 0.025 wt% $C_{16}D_mCB$ at 100,000 ppm gives the highest oil recovery over the studied formulations.

7. In oil-wet porous media, the potential for altering wettability only gives a quick recovery at the early stage. The trapped oil can only be mobilized if its capillary is reduced with the presence of low-IFT agents. Thus, wettability alteration dominants the early stage of flooding process, whereas IFT reduction is necessary for the later time recovery.

Bibliography

Abrahamsen, A. (2012). Applying Chemical EOR on the Norne Field C-Segment (Master's thesis, Institutt for petroleumsteknologi og anvendt geofysikk).

Abramov, V. O., Abramova, A. V., Bayazitov, V. M., Altunina, L. K., Gerasin, A. S., Pashin, D. M., & Mason, T. J. (2015). Sonochemical approaches to enhanced oil recovery. Ultrasonics sonochemistry, 25, 76-81.

Alotaibi, M. B., Nasr-El-Din, H. A., & Fletcher, J. J. (2011). Electrokinetics of limestone and dolomite rock particles. SPE Reservoir Evaluation & Engineering, 14(05), 594-603.

Aoudia, M., Al-Shibli, M. N., Al-Kasimi, L. H., Al-Maamari, R., & Al-bemani, A. (2006). Novel surfactants for ultralow interfacial tension in a wide range of surfactant concentration and temperature. Journal of surfactants and detergents, 9(3), 287-293.

Barnes, J. R., Smit, J., Smit, J., Shpakoff, G., Raney, K. H., & Puerto, M. (2008, January). Phase behaviour methods for the evaluation of surfactants for chemical flooding at higher temperature reservoir conditions. In SPE Symposium on Improved Oil Recovery. Society of Petroleum Engineers.

Bera, A., Mandal, A., & Guha, B. B. (2013). Synergistic effect of surfactant and salt mixture on interfacial tension reduction between crude oil and water in enhanced oil recovery. Journal of Chemical & Engineering Data, 59(1), 89-96.

Berry, J. D., Neeson, M. J., Dagastine, R. R., Chan, D. Y., & Tabor, R. F. (2015). Measurement of surface and interfacial tension using pendant drop tensiometry. Journal of colloid and interface science, 454, 226-237.

Blandamer, M. J., Cullis, P. M., Soldi, L. G., Engberts, J. B., Kacperska, A., Van Os, N. M., & Subha, M. C. S. (1995). Thermodynamics of micellar systems: comparison of mass action and phase equilibrium models for the calculation of standard Gibbs energies of micelle formation. Advances in colloid and interface science, 58(2-3), 171-209.

Bortolotti, V., Macini, P., & Srisuriyachai, F. (2009, January). Laboratory Evaluation of Alkali and Alkali-Surfactant-Polymer Flooding Combined with Intermittent Flow in Carbonatic Rocks. In Asia Pacific Oil and Gas Conference & Exhibition. Society of Petroleum Engineers.

Chen, L., Zhang, G., Wang, L., Wu, W., & Ge, J. (2014). Zeta potential of limestone in a large range of salinity. Colloids and Surfaces A: Physicochemical and Engineering Aspects, 450, 1-8.

Chevalier, Y., Storet, Y., Pourchet, S., & Le Perchec, P. (1991). Tensioactive properties of zwitterionic carboxybetaine amphiphiles. Langmuir, 7(5), 848-853.

Chu, Y. P., Gong, Y., Tan, X. L., Zhang, L., Zhao, S., An, J. Y., & Yu, J. Y. (2004). Studies of synergism for lowering dynamic interfacial tension in sodium α-(n-alkyl) naphthalene sulfonate/alkali/acidic oil systems. Journal of colloid and interface science, 276(1), 182-187.

Craig, F. F. (1971). The reservoir engineering aspects of waterflooding (Vol. 3, pp. 45-47). New York: HL Doherty Memorial Fund of AIME.

Dahami, M. A., Constant, W. D., & Wolcott, J. M. (1988). Alcohol-assisted alkaline flooding for enhanced oil recovery. Fuel, 67(9), 1242-1248.

Donaldson, E. C., & Alam, W. (2013). Wettability. Elsevier.

Dong, M., Ma, S., & Liu, Q. (2009). Enhanced heavy oil recovery through interfacial instability: A study of chemical flooding for Brintnell heavy oil. Fuel, 88(6), 1049-1056.

Dubey, S. T., & Doe, P. H. (1993). Base number and wetting properties of crude oils. SPE Reservoir Engineering, 8(03), 195-200.

Dwarakanath, V., Chaturvedi, T., Jackson, A., Malik, T., Siregar, A. A., & Zhao, P. (2008, January). Using co-solvents to provide gradients and improve oil recovery during chemical flooding in a light oil reservoir. In SPE Symposium on Improved Oil Recovery. Society of Petroleum Engineers.

El-Batanoney, M., Abdel-Moghny, T., & Ramzi, M. (1999). The effect of mixed surfactants on enhancing oil recovery. Journal of Surfactants and Detergents, 2(2), 201-205.

Fakhari, A., Corcoran, M., & Schwarz, A. (2017). Thermogelling properties of purified poloxamer 407. Heliyon, 3(8), e00390.

Fuseni, A., Han, M., & Al-Mobith, A. (2013, May). Phase behavior and interfacial tension properties of an amphoteric surfactant for EOR application. In SPE Saudi Arabia section technical symposium and exhibition. Society of Petroleum Engineers.

Gao, B., & Sharma, M. M. (2013). A family of alkyl sulfate gemini surfactants. 2. Water–oil interfacial tension reduction. Journal of colloid and interface science, 407, 375-381.

Ge, J., & Wang, Y. (2015). Surfactant enhanced oil recovery in a high temperature and high salinity carbonate reservoir. Journal of Surfactants and Detergents, 18(6), 1043-1050.

Gogarty, W. B., & Tosch, W. C. (1968). Miscible-type waterflooding: oil recovery with micellar solutions. Journal of Petroleum Technology, 20(12), 1-407.

Guo, S., Wang, H., Shi, J., Pan, B., & Cheng, Y. (2015). Synthesis and properties of a novel alkyl-hydroxyl-sulfobetaine zwitterionic surfactant for enhanced oil recovery. Journal of Petroleum Exploration and Production Technology, 5(3), 321-326.

Gupta, R., & Mohanty, K. K. (2008, January). Wettability alteration of fractured carbonate reservoirs. In SPE Symposium on Improved Oil Recovery. Society of Petroleum Engineers.

Hirasaki, G. J. (1991). Wettability: fundamentals and surface forces. SPE Formation Evaluation, 6(02), 217-226.

Hirasaki, G., Miller, C. A., & Puerto, M. (2011). Recent advances in surfactant EOR. SPE Journal, 16(04), 889-907.

Hongyan, W., Xulong, C., Jichao, Z., & Aimei, Z. (2009). Development and application of dilute surfactant–polymer flooding system for Shengli oilfield. Journal of Petroleum Science and Engineering, 65(1-2), 45-50.

Iglauer, S., Wu, Y., Shuler, P., Tang, Y., & Goddard III, W. A. (2009). Alkyl polyglycoside surfactant–alcohol cosolvent formulations for improved oil recovery. Colloids and Surfaces A: Physicochemical and Engineering Aspects, 339(1-3), 48-59.

Iglauer, S., Wu, Y., Shuler, P., Tang, Y., & Goddard III, W. A. (2011). Alkyl polyglycoside/1-naphthol formulations: a case study of surfactant enhanced oil recovery. Tenside Surfactants Detergents, 48(2), 121-126.

Jackson, M. D., Al-Mahrouqi, D., & Vinogradov, J. (2016). Zeta potential in oil-water-carbonate systems and its impact on oil recovery during controlled salinity water-flooding. Scientific reports, 6, 37363.

James-Smith, M. A., Alford, K., & Shah, D. O. (2007). A novel method to quantify the amount of surfactant at the oil/water interface and to determine total interfacial area of emulsions. Journal of colloid and interface science, 310(2), 590-598.

Kamal, M. S., Hussein, I. A., & Sultan, A. S. (2017). Review on surfactant flooding: phase behavior, retention, IFT, and field applications. Energy & Fuels, 31(8), 7701-7720.

Kamal, M. S., Shakil Hussain, S. M., & Fogang, L. T. (2018). A zwitterionic surfactant bearing unsaturated tail for enhanced oil recovery in high-temperature high-salinity reservoirs. Journal of Surfactants and Detergents, 21(1), 165-174.

Kamil, M., & Siddiqui, H. (2013). Experimental study of surface and solution properties of gemini-conventional surfactant mixtures on solubilization of polycyclic aromatic hydrocarbon. Modeling and Numerical Simulation of Material Science, 3(04), 17.

Karambeigi, M. S., Abbassi, R., Roayaei, E., & Emadi, M. A. (2015). Emulsion flooding for enhanced oil recovery: interactive optimization of phase behavior, microvisual and core-flood experiments. Journal of Industrial and Engineering Chemistry, 29, 382-391.

Karnanda, W., Benzagouta, M. S., AlQuraishi, A., & Amro, M. M. (2013). Effect of temperature, pressure, salinity, and surfactant concentration on IFT for surfactant flooding optimization. Arabian Journal of Geosciences, 6(9), 3535-3544.

Kumar, A., & Mandal, A. (2018). Characterization of rock-fluid and fluid-fluid interactions in presence of a family of synthesized zwitterionic surfactants for application in enhanced oil recovery. Colloids and Surfaces A: Physicochemical and Engineering Aspects, 549, 1-12.

Kumar, S., Panigrahi, P., Saw, R. K., & Mandal, A. (2016). Interfacial interaction of cationic surfactants and its effect on wettability alteration of oil-wet carbonate rock. Energy & Fuels, 30(4), 2846-2857.

Lager, A., Webb, K. J., Black, C. J. J., Singleton, M., & Sorbie, K. S. (2008). Low salinity oil recovery-an experimental investigation1. Petrophysics, 49(01).

Li, G. Z., Mu, J. H., Li, Y., & Yuan, S. L. (2000). An experimental study on alkaline/surfactant/polymer flooding systems using nature mixed carboxylate. Colloids and Surfaces A: Physicochemical and Engineering Aspects, 173(1-3), 219-229.

Ligthelm, D. J., Gronsveld, J., Hofman, J., Brussee, N., Marcelis, F., & van der Linde, H. (2009, January). Novel waterflooding strategy by manipulation of injection brine composition. In EUROPEC/EAGE conference and exhibition. Society of Petroleum Engineers.

Lv, W., Bazin, B., Ma, D., Liu, Q., Han, D., & Wu, K. (2011). Static and dynamic adsorption of anionic and amphoteric surfactants with and without the presence of alkali. Journal of Petroleum Science and Engineering, 77(2), 209-218.

Ma, K., Cui, L., Dong, Y., Wang, T., Da, C., Hirasaki, G. J., & Biswal, S. L. (2013). Adsorption of cationic and anionic surfactants on natural and synthetic carbonate materials. Journal of colloid and interface science, 408, 164-172.

Mafi, A., Hu, D., & Chou, K. C. (2016). Interactions of sulfobetaine zwitterionic surfactants with water on water surface. Langmuir, 32(42), 10905-10911.

Mahani, H., Keya, A. L., Berg, S., & Nasralla, R. (2017). Electrokinetics of carbonate/brine interface in low-salinity waterflooding: Effect of brine salinity, composition, rock type, and pH on ζ-potential and a surface-complexation model. SPE Journal, 22(01), 53-68.

Mahani, H., Keya, A. L., Berg, S., Bartels, W. B., Nasralla, R., & Rossen, W. R. (2015). Insights into the mechanism of wettability alteration by low-salinity flooding (LSF) in carbonates. Energy & Fuels, 29(3), 1352-1367.

Manrique, E. J., Muci, V. E., & Gurfinkel, M. E. (2007). EOR field experiences in carbonate reservoirs in the United States. SPE Reservoir Evaluation & Engineering, 10(06), 667-686.

Matsuno, R., Takami, K., & Ishihara, K. (2010). Simple synthesis of a library of zwitterionic surfactants via Michael-type addition of methacrylate and alkane thiol compounds. Langmuir, 26(16), 13028-13032.

Morvan, M., Moreau, P., Degre, G., Leng, J., Masselon, C., Bouillot, J., & Zaitoun, A. (2009, January). New viscoelastic fluid for chemical EOR. In SPE international symposium on oilfield chemistry. Society of Petroleum Engineers.

Mosayeb, A., & Abedini, R. (2012). The effect of non-ionic surfactants on the interfacial tension between crude oil and water. Petroleum & Coal, 54(2).

Nilsson, S., Lohne, A., & Veggeland, K. (1997). Effect of polymer on surfactant floodings of oil reservoirs. Colloids and Surfaces A: Physicochemical and Engineering Aspects, 127(1-3), 241-247.

Okamoto, T., Tomomasa, S., & Nakajima, H. (2016). Preparation and thermal properties of fatty alcohol/surfactant/oil/water nanoemulsions and their cosmetic applications. Journal of oleo science, 65(1), 27-36.

Pal, S., Mushtaq, M., Banat, F., & Al Sumaiti, A. M. (2018). Review of surfactant-assisted chemical enhanced oil recovery for carbonate reservoirs: challenges and future perspectives. Petroleum Science, 15(1), 77-102.

Pei, H., Zhang, G., Ge, J., Zhang, L., & Ma, M. (2014). Effect of the addition of low molecular weight alcohols on heavy oil recovery during alkaline flooding. Industrial & Engineering Chemistry Research, 53(4), 1301-1307.

Pope, G. A., Tsaur, K., Schechter, R. S., & Wang, B. (1982). The effect of several polymers on the phase behavior of micellar fluids. Society of Petroleum Engineers Journal, 22(06), 816-830.

Qi, L., Fang, Y., Wang, Z., Ma, N., Jiang, L., & Wang, Y. (2008). Synthesis and physicochemical investigation of long alkylchain betaine zwitterionic surfactant. Journal of Surfactants and Detergents, 11(1), 55-59.

Quan, X., Jiazhong, W., Jishun, Q., Qingjie, L., Desheng, M., Li, L., & Manli, L. (2012, August). Investigation of electrical surface charges and wettability alteration by ions matching waterflooding. In International Symposium of the Society of Core Analysts, Aberdeen, Scotland (pp. 27-30).

Roehl, P. O., & Choquette, P. W. (Eds.). (2012). Carbonate petroleum reservoirs. Springer Science & Business Media.

Sahni, V., Dean, R. M., Britton, C., Kim, D. H., Weerasooriya, U., & Pope, G. A. (2010, January). The role of co-solvents and co-surfactants in making chemical floods robust. In SPE Improved Oil Recovery Symposium. Society of Petroleum Engineers.

Sakamoto, K., Lochhead, R., Maibach, H., & Yamashita, Y. (Eds.). (2017). Cosmetic science and technology: theoretical principles and applications. Elsevier.

Salter, S. J. (1977, January). The influence of type and amount of alcohol on surfactant-oil-brine phase behavior and properties. In SPE Annual Fall Technical Conference and Exhibition. Society of Petroleum Engineers.

Salter, S. J. (1978, January). Selection of pseudo-components in surfactant-oil-brine-alcohol systems. In SPE Symposium on Improved Methods of Oil Recovery. Society of Petroleum Engineers.

Sandengen, K., Tweheyo, M. T., Raphaug, M., Kjølhamar, A., Crescente, C., & Kippe, V. (2011, September). Experimental evidence of low salinity water flooding yielding a more oil-wet behaviour. In Proceedings of the International Symposium of the Society of Core Analysts (pp. 18-21).

Sandersen, S. B., Stenby, E. H., & von Solms, N. (2012). Enhanced oil recovery with surfactant flooding.

Seethepalli, A., Adibhatla, B., & Mohanty, K. K. (2004). Physicochemical interactions during surfactant flooding of fractured carbonate reservoirs. SPE journal, 9(04), 411-418.

Seredyuk, V., Alami, E., Nyden, M., Holmberg, K., Peresypkin, A. V., & Menger, F. M. (2001). Micellization and adsorption properties of novel zwitterionic surfactants. Langmuir, 17(17), 5160-5165.

Shabani Afrapoli, M., Alipour, S., & Torsaeter, O. (2010, January). Effect of wettability and interfacial tension on microbial improved oil recovery with Rhodococcus sp 094. In SPE Improved Oil Recovery Symposium. Society of Petroleum Engineers.

Shah, D. O. (Ed.). (1981). Surface phenomena in enhanced oil recovery (pp. 53-72). New York: Plenum Press.

Sheng, J. (Ed.). (2013). Enhanced oil recovery field case studies. Gulf Professional Publishing.

Sheng, J. J. (2015). Status of surfactant EOR technology. Petroleum, 1(2), 97-105.

Siggel, L., Santa, M., Hansch, M., Nowak, M., Ranft, M., Weiss, H., ... & Tinsley, J. (2012, January). A new class of viscoelastic surfactants for enhanced oil recovery. In SPE Improved Oil Recovery Symposium. Society of Petroleum Engineers.

Singh, R. (2011). Solubilization of organic dyes in surfactant micelles.

Skauge, A., Garnes, J. M., Mørner, O. J., & Torske, L. (1992). Optimization of a surfactant flooding process by core-flood experiments. Journal of Petroleum Science and Engineering, 7(1-2), 117-130.

Speight, J. G. (2016). Introduction to enhanced recovery methods for heavy oil and tar sands. Gulf Professional Publishing.

Standnes, D. C., & Austad, T. (2000). Wettability alteration in chalk: 2. Mechanism for wettability alteration from oil-wet to water-wet using surfactants. Journal of Petroleum Science and Engineering, 28(3), 123-143.

Standnes, D. C., & Austad, T. (2003). Wettability alteration in carbonates: Interaction between cationic surfactant and carboxylates as a key factor in wettability alteration from oil-wet to water-wet conditions. Colloids and Surfaces A: Physicochemical and Engineering Aspects, 216(1-3), 243-259.

Suniga, P. T., Fortenberry, R., & Delshad, M. (2016, April). Observations of microemulsion viscosity for surfactant EOR processes. In SPE Improved Oil Recovery Conference. Society of Petroleum Engineers.

Taber, J. J., Martin, F. D., & Seright, R. S. (1997). EOR screening criteria revisited-Part 1: Introduction to screening criteria and enhanced recovery field projects. SPE Reservoir Engineering, 12(03), 189-198.

Taylor, K. C., & Nasr-El-Din, H. A. (1996). The effect of synthetic surfactants on the interfacial behaviour of crude oil/alkali/polymer systems. Colloids and Surfaces A: Physicochemical and Engineering Aspects, 108(1), 49-72.

Telmadarreie, A., & Trivedi, J. J. (2016). New insight on carbonate-heavy-oil recovery: pore-scale mechanisms of post-solvent carbon dioxide foam/polymer-enhanced-foam flooding. SPE Journal, 21(05), 1-655.

Thomas, M. M., Clouse, J. A., & Longo, J. M. (1993). Adsorption of organic compounds on carbonate minerals: 1. Model compounds and their influence on mineral wettability. Chemical Geology, 109(1-4), 201-213.

Trabelsi, S., Hutin, A., Argillier, J. F., Dalmazzone, C., Bazin, B., & Langevin, D. (2012). Effect of added surfactants on the dynamic interfacial tension behaviour of alkaline/diluted heavy crude oil system. Oil & Gas Science and Technology–Revue d'IFP Energies nouvelles, 67(6), 963-968.

Vonnegut, B. (1942). Rotating bubble method for the determination of surface and interfacial tensions. Review of scientific instruments, 13(1), 6-9.

Wei, B., Lu, L., Li, Q., Li, H., & Ning, X. (2017). Mechanistic study of oil/brine/solid interfacial behaviors during low-salinity waterflooding using visual and quantitative methods. Energy & Fuels, 31(6), 6615-6624.

Wu, X., Han, M., Zahrani, B. H., & Guo, L. (2015, March). Effect of surfactant-polymer interaction on the interfacial properties for chemical EOR. In SPE Middle East Oil & Gas Show and Conference. Society of Petroleum Engineers.

Wu, Y. A., Iglauer, S., Shuler, P., Tang, Y., & Goddard III, W. A. (2010). Branched alkyl alcohol propoxylated sulfate surfactants for improved oil recovery. Tenside Surfactants Detergents, 47(3), 152-161.

Xie, D., Hou, J., Zhao, F., & Doda, A. (2016). The comparison study of IFT and consumption behaviors between organic alkali and inorganic alkali. Journal of Petroleum Science and Engineering, 147, 528-535.

Yang, H. T., Britton, C., Liyanage, P. J., Solairaj, S., Kim, D. H., Nguyen, Q. P., ... & Pope, G. A. (2010, January). Low-cost, high-performance chemicals for enhanced oil recovery. In SPE Improved Oil Recovery Symposium. Society of Petroleum Engineers.

Yarveicy, H., & Javaheri, A. (2017). Application of Lauryl Betaine in enhanced oil recovery: A comparative study in micromodel. Petroleum.

Yoshimura, T., Ichinokawa, T., Kaji, M., & Esumi, K. (2006). Synthesis and surface-active properties of sulfobetaine-type zwitterionic gemini surfactants. Colloids and Surfaces A: Physicochemical and Engineering Aspects, 273(1-3), 208-212.

Zdziennicka, A., & Jańczuk, B. (2017). Thermodynamic parameters of some biosurfactants and surfactants adsorption at water-air interface. Journal of Molecular Liquids, 243, 236-244.

Zhang, L., Luo, L., Zhao, S., & Yu, J. (2002). Studies of synergism/antagonism for lowering dynamic interfacial tensions in surfactant/alkali/acidic oil systems, part 2: synergism/antagonism in binary surfactant mixtures. Journal of colloid and interface science, 251(1), 166-171.

Zhang, S., Xu, Y., Qiao, W., & Li, Z. (2004). Interfacial tensions upon the addition of alcohols to phenylalkane sulfonate monoisomer systems. Fuel, 83(14-15), 2059-2063.

Zhao, G., Khin, C. C., Chen, S. B., & Chen, B. H. (2005). Nonionic surfactant and temperature effects on the viscosity of hydrophobically modified hydroxyethyl cellulose solutions. The Journal of Physical Chemistry B, 109(29), 14198-14204.

Zhao, J., Dai, C., Ding, Q., Du, M., Feng, H., Wei, Z., ... & Zhao, M. (2015). The structure effect on the surface and interfacial properties of zwitterionic sulfobetaine surfactants for enhanced oil recovery. RSC Advances, 5(18), 13993-14001.

Zhao, P., Jackson, A., Britton, C., Kim, D. H., Britton, L. N., Levitt, D., & Pope, G. A. (2008, January). Development of high-performance surfactants for difficult oils. In SPE Symposium on Improved Oil Recovery. Society of Petroleum Engineers.

Zhao, Z., Bi, C., Li, Z., Qiao, W., & Cheng, L. (2006). Interfacial tension between crude oil and decylmethylnaphthalene sulfonate surfactant alkali-free flooding systems. Colloids and Surfaces A: Physicochemical and Engineering Aspects, 276(1-3), 186-191.